

qNMR fluorine pollution analysis: perspectives on PFAS exposure characterisation using ^{19}F NMR

Laura Ducié¹ , Julia Asencio Hernandez¹ ,

Marc-André Delsuc² , Anne Briot-Dietsch¹ *

¹ CASC4DE NMR lab, Illkirch, France

² IGBMC, Illkirch, France

* Corresponding author: anne.briot-dietsch@casc4de.eu

24 April 2025

Abstract

The presence of anthropogenic fluorinated pollutants in the environment, particularly per- and polyfluoroalkyl substances (PFAS), is an increasing concern. The need for untargeted analytical methods is becoming increasingly critical to comprehensively assess environmental contamination. Classical approaches include targeted searches for marker molecules, for which standard references must be available or total fluorine estimation without individual species identification. Given the diversity of commercially compounds, and their possible degradation products, it appears impossible to obtain a global view of environmental fluorinated species.

We present investigation to highlight the potential of liquid state ^{19}F -Nuclear Magnetic Resonance (NMR) using broadband acquisition and advocate it as a complementary untargeted routine strategy for obtaining additional information alongside existing methods. We introduce a repertoire of 1D and 2D NMR experiments allowing to quantify efficiently all detected fluorinated molecules in a given matrix. The specific problems of ^{19}F -NMR at high magnetic field are exposed, notably the difficulty of exciting and detecting a large broadband spectral width tackled thanks to adapted pulse sequences. Acquisition parameters have been optimized for quantification accuracy and robustness of the proposed techniques against miss-calibration. Despite limited sensitivity compared to others approaches, ^{19}F -NMR insures minimal sample treatment and few handling constraints.

Through real-world case studies from consumer products to PFAS-contaminated environments, we demonstrate that ^{19}F -NMR is not only suitable for quantification, but a powerful tool for the comprehensive detection of both known and unexpected fluorinated species in environmental samples, with for instance LOD down to 20 µg/L for trifluoroacetic acid (TFA).

Keywords

^{19}F NMR, fluorinated pollutants diagnosis, PFAS, nontarget analysis, broadband NMR, quantitative NMR, total organic fluorine

Abbreviations Please note that PFAS Abbreviations stands for per- and polyfluoroalkyl substances, including their acid forms, salts, and related substances; AFFF, aqueous film forming foam; ANSES, agence nationale de sécurité sanitaire de l'alimentation, de l'environnement et du travail; AOF, adsorbable organic fluorine; CEC, contaminant of emerging concern; CIC, combustion ion chromatography; COSY, correlated spectroscopy; DMSO, dimethyl sulfoxide; DOSY, diffusion ordered spectroscopy; ECHA, European chemicals agency; EOF, extractable organic fluorine; FASA, perfluoroalkyl sulfonamide; FID, free induction decay; FTCA, fluorotelomer carboxylic acid; FTOH, fluorotelomer alcohol; FTSA, fluorotelomer sulfonic acid; HFPO-DA, hexafluoropropylene oxide-dimer acid, 2,3,3,3-tetrafluoro-2-(heptafluoropropoxy)propanoic acid or chemicals from GenX trademark also known as FRD-903; HFPO-TA, hexafluoropropylene oxide-trimer acid, perfluoro-2,5-dimethyl-3,6-dioxanonanoic acid; HFPO-TeA, hexafluoropropylene oxide tetramer acid; HMQC, heteronuclear multiple quantum correlation; LC-MS/MS, liquid chromatography coupled to tandem mass spectrometry; LED, longitudinal eddy delay; LOD, limit of detection; LOQ, limit of quantification; MS, mass spectrometry;

NMR, nuclear magnetic resonance; OECD, organisation for economic co-operation and development; PFAS, poly- and perfluorinated substance; PFBA, perfluorinated butyric acid; PFCA, perfluorinated carboxylic acid; PFECA, perfluoropolyether carboxylic acid; PFG, pulsed field gradient; PFHxS, perfluorohexanesulfonic acid; PFMOPrA, perfluoro-3-methoxypropanoic acid; PFOA, perfluorooctanoic acid; PFOS, perfluorooctanesulfonic acid; PFPA, perfluorinated phosphonic acid; PFSA, perfluorinated sulfonic acid; PTFE, polytetrafluoroethylene; POP, persistent organic pollutant; qNMR, quantitative nuclear magnetic resonance; REACH, registration, evaluation, authorisation and restriction of chemicals; SNR, signal to noise ratio; SPIKE, spectrometry processing innovative kernel; SOFAST, selective optimized flip angle short transient; SW, spectral width; TFA, trifluoroacetic acid; UNEP, United Nations environment programme; USEPA, United States environmental protection agency.

1 Fluorine world

1.1 A small but strong element

Fluorine is a key element, more abundant in the Earth's crust than sulfur or zinc. It is unknown to the biologist because there is nearly no fluorine metabolism in any living organism. To the chemist, it is however a favourite element, with the highest electronegativity and a strong C-F bond that provides specific properties and extreme resistance to harsh conditions.¹ Due to these characteristics, fluorine has occupied a unique place in the chemist's toolbox over the past century.² Indeed, the use of fluorine in pharmaceutical, agrochemical, and repellent or nonstick finishes industries has been extensively developed since at least the 1950's.

Today Solvay, a major player in the chemical industry, estimates that "ca. 30% of drugs and 50% of crop protection products under development contain fluorine".³ Indeed, it is already present inside our houses in the form of drugs such as antibiotics ciprofloxacin (Ciflox®, Cipro®) or levofloxacin (Levaquin®, Tavanic®), nonsteroidal anti-inflammatory drugs niflumic acid (Nifluril®) or celecoxib (Celebrex®), antidepressant fluoxetine (Prozac®), seasonal allergic rhinitis relieving fluticasone propionate (Dymista®) and the lipid lowering agent atorvastatin (Lipitor®)... Roughly one in five medications currently on the market are fluoropharmaceuticals.^{4; 5; 6; 7} Regarding agrochemical products newly developed in the last decade more than 60% contain a fluorine moiety.^{8; 9} Not to mention its historical use in poly- and perfluorinated substances (PFAS) and derivated polymer films and membranes blockbusters Teflon®, Nafion®, Scotchgard® (Figure 1)...

1.2 PFAS, the « Forever Chemicals »

PFAS are a class of synthetic fluorine-based chemicals¹⁰ closely scrutinized, used in high-tech applications but now considered to be toxic environmental pollutants and designated as contaminants of emerging concern (CEC) and persistent organic pollutants (POP).^{11; 12}

Discovered in the 1930's, their usage went largely unregulated until the early 2000's.¹³ Due to characteristics of fluorine, these poly- and perfluorinated substances show remarkable repellent or nonstick properties which are widely used by the industry in everyday objects: water repellent gear, stain resistant fabric, food packaging, non-stick cookware, personal care products, Aqueous Film-Forming Foam (AFFF) used for firefighting.^{13; 14} Applications extend across multiple sectors.¹⁵ First used in the military field during the Second World War, in connection with work on the atomic bomb, PFAS have subsequently fuelled significant industrial development, with numerous civil and domestic applications.^{16; 17} The use of perfluorinated compound into materials has enhanced their performance providing exceptional chemical resistance and impermeability. They are even used in environmental engineering solutions such as landfill liners, storage tanks, and industrial barriers designed to prevent soil and groundwater contamination.¹⁴

Among emblematic compounds are perfluorooctanoic acid (PFOA), primary ingredient in Teflon®, perfluorooctanesulfonic acid (PFOS), historical component of Scotchgard®, and then the fluoroether, hexafluoropropylene oxide-dimer acid (HFPO-

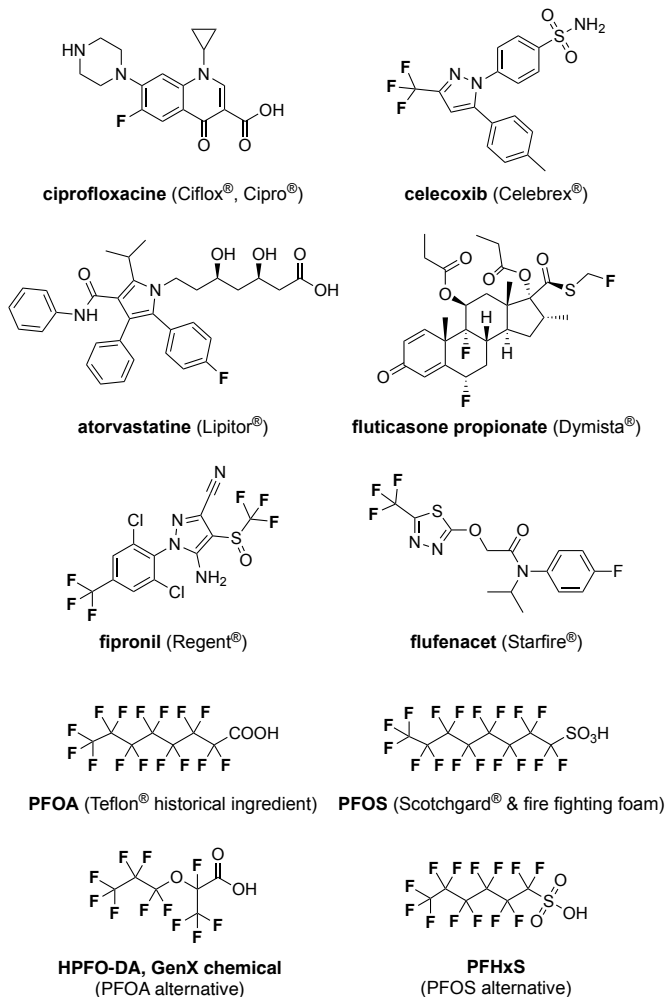


Figure 1. Molecular structure of some typical man-made fluorinated compounds: medicines; agrochemicals; historical perfluorinated compounds used in polymer films applications, i.e. perfluorooctanoic acid (PFOA) and perfluorooctanesulfonic acid (PFOS); their shorter-chain alternatives, i.e. hexafluoropropylene oxide-dimer acid (HFPO-DA) and perfluorohexanesulfonic acid (PFHxS).

DA) and its ammonium salt referred to as "GenX chemicals", developed as a safer alternative but finally more toxic than the PFOA they were supposed to replace^{18; 19} and leading to the so-called regrettable substitution phenomenon²⁰ (Figure 1). It is estimated that "more than a megaton of PFAS is produced yearly, and thousands of PFAS wind up in end-use products",²¹ and that "around 4.4 million tonnes of PFAS would end up in the environment over the next 30 years unless action is taken".²²

As of today, more than 10 000 highly fluorinated compounds have been inventoried by the United States environmental protection agency (USEPA)²³ and proposed in early 2023 for restriction by European chemicals agency (ECHA).²² The original 2018 definition of the organisation for economic co-operation and development (OECD) defined PFAS as molecules containing three or more fully fluorinated carbons connected to each other or two such carbons linked by

an ether group. In 2021, the USEPA broadened this definition to also include compounds with two adjacent fluorinated carbon.

As highly fluorinated PFAS are thermally and chemically stable, they are resistant to most biological and chemical degradation mechanisms.²⁴ Therefore, these compounds have accumulated in ecosystems. They are considered as POP as either because they are persistent themselves or degrade to persistent PFAS. Environmental studies have already shown the presence of PFAS in soil, sediments, water resources and wildlife, leading to a growing awareness of their omnipresence.^{25; 26; 27} As a result of inadequate environmental assessment frameworks for their monitoring, their study and surveillance are relatively recent, even though they have been accumulating in the environment for a longer time. They are recognized as a major environmental and health problem of global dimension. Indeed, all these molecules share a common feature: they present a toxicity at relatively low concentrations with confirmed impacts on human health, e.g. carcinogenic, endocrine disrupting, reprotoxic, lowering birth weight, accelerating puberty, affecting immunity and thyroid activity, reducing vaccine response, damaging the liver and kidney, leading to lipid and insulin dysregulation.^{28; 29; 30}

Despite intensive works worldwide,^{31; 32; 30} the harsh reality remains that there is no global remediation solution right now, even new interesting approach to PFAS management have recently emerged.³³ Thus, their accumulation in the environment and their potential for water or food contamination raise concerns regarding their impact on human health. Motivated by these concerns, regulations have emerged. In 2001 the Stockholm Convention initiated by the United Nations Environment Programme (UNEP) Governing Council has set guidelines to mitigate POP and has started to enforce restrictions on PFOS (2009), on PFOA (2020) and on perfluorohexanesulfonic acid (PFHxS) (2022).³⁴ Now long-chain (C9-21) perfluorinated carboxylic acids (PFCA) are also being considered for inclusion. At European level, regulation on the registration, evaluation, authorization, and restriction of chemicals (REACH) has occurred for C9-14 PFCA and derivatives in 2023 and now other PFAS are under evaluation.³⁵ Since August 2023 the PFHxS group has been restricted by the European POP Regulation. In United States, since 2021, a framework "PFAS Strategic Roadmap" was set by the USEPA detailing the agency's regulatory plans from 2021 to 2024.³⁶

Although scientists have now identified key points to address the "PFAS problem",^{29; 37; 38} a real engagement of all stakeholders—including scientists, consumers, authorities, and manufacturers—is crucial to contain the magnitude of the issue.³⁹

Interestingly, the definition of PFAS remains a contentious issue. In 2021, the OECD further broadened the definition to include any compound containing at least one CF₃ (trifluoromethyl) or CF₂ (difluoromethylene) group.⁴⁰ This evolution drastically increases the number of recognized PFAS, now estimated at nearly 15,000 compounds with this definition. This reclassification means that many fluorinated pesticides, like flufenacet, fipronil, flurochloridone, flutianil, isoxaflutole, penthiopyrad, pyroxsulam... now fall within the PFAS family. However, some advocate for a narrower focus on molecules with many fluorine atoms, as these often exhibit specific properties that make PFAS persistent and hazardous.

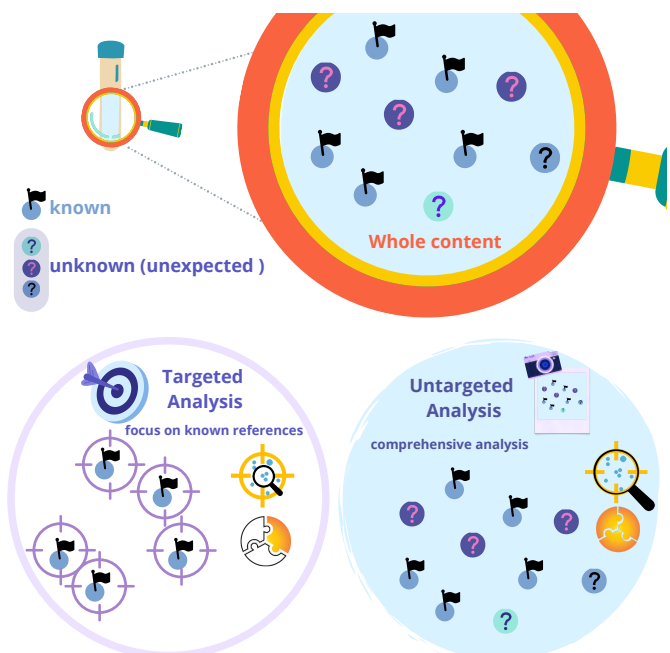


Figure 2. Targeted versus untargeted approach for in-depth fluorine content exploration. Untargeted approach is appropriate to detect unexpected compounds and reduces biases as no prior knowledge about the sample is needed. It can reveal the presence of unexpected compounds that might be overlooked in a targeted analysis. However the challenge lies in the identification process.

1.3 Fluorine pollution challenge

Fluorinated compounds, including PFAS, which have been introduced to the market in large numbers, have a significant impact on the environment. Over the past three decades, the detection of these compounds in ecosystems and the understanding of their hazardous effects have become more pronounced characterizing pollution issues.^{41; 42} Overall the regulatory landscape is evolving positively around the world to assess and mitigate their environmental and health impacts.

However, to address existing issues, and to comprehensively assess and map risks, it is necessary to have a robust, untargeted, holistic, easy-to-handle approach allowing analyses in number. Pollution analysis is a complex issue that demands handling an extensive diversity of pollutant species (known, emerging, all continually being identified) and few scientific knowledge about their toxicity⁴³. This approach has to deal with extreme concentrations (very low or very high ones), requiring either highly sensitive or robust detection methods for heavily contaminated samples. Large data collections are needed as well to accurately assess pollution levels and sources as environmental conditions can significantly vary and affect dispersion and concentration. Finally, potential matrix effects on detection and quantification of the targeted pollutants may require prior complex sample preparation and purification techniques.⁴⁴ Addressing these challenges is crucial for accurate pollution assessment and further effective remediation.

Targeted and untargeted analysis methods are the two approaches in analytical chemistry, each serving distinct purposes in the identification and quantification of compounds

(Figure 2). On the one hand, targeted approach is more of *a priori* knowledge method since it involves measuring a predetermined set of previously characterized analytes. While it facilitates the optimization of analytical protocols, it performs badly in adapting to the multiple potential scenarios of PFAS and fluorochemicals pollution. On the other hand, untargeted approach is a global and comprehensive measurement of both known and unknown compounds. It involves investigating pollution as a whole, even if this may necessitate making assumptions and raising challenging identification issues.

Currently, there is no complete untargeted technique for detecting, identifying and quantifying PFAS and fluorochemical pollutants. Existing routines primarily rely on Liquid Chromatography coupled with tandem Mass Spectrometry (LC-MS/MS).^{45; 46; 47; 48; 49; 50} This targeted approach encounters challenges such as the limited availability of authentic reference standards, approximately 150 for PFAS as of today compared to the estimated 10,000 existing PFAS compounds. LC-MS/MS methods are also facing troubles such as time-consuming preparations, treatments that may alter sample content, matrix effects, sample extraction limited by solvents mixture compatibility or overly contaminated samples.^{44; 51} On the positive side, the Limit of Quantification (LOQ) of LC-MS/MS typically reaches the low- ng/L and low- ng/g range, except for surface water, where it is usually sub-50 ng/L , and for wastewater or effluents, where it is often sub-100 ng/L , due to interference from matrix components. In fact, LOQ typically depends on the instrument, the specific PFAS being analysed, and the sample matrix. Short-chain PFAS, like perfluorinated butyric acid (PFBA), often have higher LOQ due to their lower ionization efficiency. Regarding suspect screening using high-resolution mass spectrometry to detect known PFAS without requiring reference standards, the approach bridges targeted and non-targeted analysis to identify PFAS based on accurate mass, retention time, and MS/MS fragmentation patterns. It can allow for detecting more fluorinated compounds beyond the limited list covered by targeted methods.⁵² Nevertheless it remains suspect list dependent, and involves complex data processing and limited structural confirmation (isomers).

In contrast, untargeted methods, relying on adsorptive phases like Adsorbable Organic Fluorine (AOF)⁵³ or Extractable Organic Fluorine (EOF) and use combustion ion chromatography (CIC) to mineralize and quantify organic fluorine, provide a broad screening approach for detecting fluorinated organic compounds (and eventually residual inorganic fluoride not removed during preparation).⁵⁴ EOF, using a polymeric cartridge (e.g., weak anion exchange type) as the adsorbing phase and suitable solvents, can offer insights on a broad range of fluorinated species. AOF provides a collective assessment of all fluorinated compounds that can adsorb onto activated carbon, including PFAS, and captures all those not specifically regulated or less studied, and is expected to minimize the co-extraction of inorganic fluorides. However, the lack of specificity of these sum parameters means that they cannot identify which particular PFAS or fluorinated compounds are present, making it impossible to provide detailed risk assessments. Furthermore, they are limited by matrix effects, such as interference from complex samples like wastewater or soil and are unable to detect non-adsorbable or volatile fluorinated compounds. The LOQ of AOF and EOF depends on the specific analytical method, instrumentation,

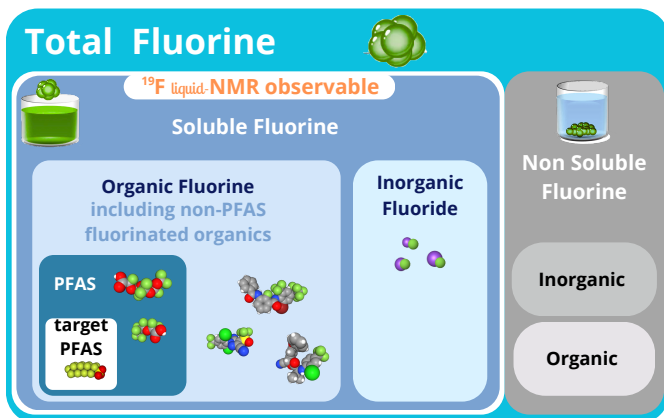


Figure 3. Diagram illustrating total fluorine analysis, highlighting the partitioning of fluorine species in a sample. Soluble fractions are observable by ^{19}F NMR, distinguishing PFAS within the soluble fraction and target PFAS typically analysed via LC-MS/MS.

and sample preparation process. Commonly these LOQ are in the range of sub- $\mu\text{g}/\text{L}$ in aqueous matrices (e.g., drinking water, groundwater, or wastewater).

As of today, there is a critical need for a method that not only targets individual chemicals but allows detection of total fluorinated content: PFAS and eventually unexpected others non-PFAS fluorinated contaminants or metabolites present in the sample^{29; 55} and quantification of total fluorine parameter⁵⁶ (Figure 3). Ideally, this technique should be highly selective, i.e. targeting only PFAS while excluding inorganic fluoride species, and comprehensive, capable of detecting thousands of known and unknown PFAS with sufficient recovery rates. In the present work, we propose to consider ^{19}F nuclear magnetic resonance (NMR) as a possible approach for untargeted analysis to detect the presence of fluorinated and perfluorinated species. In addition, ^{19}F NMR can offer valuable structural information, offering a more comprehensive understanding of contamination profiles by revealing information about the implied species families. Such an approach could facilitate the identification of broader contamination patterns and contribute to more effective site prioritization and investigation strategies.

2 NMR Approach of fluorine pollution diagnosis

2.1 ^{19}F NMR, a powerful spectroscopy

Based on the magnetic properties of certain atomic nuclei, NMR spectroscopy is a powerful analytical technique to unlock physical, chemical, and biological properties of matter,^{57; 58; 59} from small organic molecules to complex biomolecules and advanced materials. Because of its versatility and precision, NMR is increasingly being recognized in the development of international standards.⁶⁰

NMR covers a broad range of molecules and provides access to the molecular diversity while being inherently quantitative, and naturally untargeted. While the properties of NMR active nuclei such as ^1H , ^{13}C or ^{31}P may be familiar to the reader, the ^{19}F was one of the very first spins studied in the 1950s⁵⁷ and ^{19}F spectroscopy presents some specificities which are presented below.

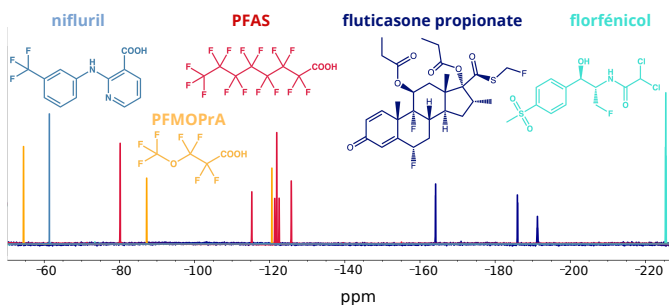


Figure 4. The large dispersion of chemical shifts in fluorine NMR for example from ca. -55 ppm for $-\text{OCF}_3$ groups of perfluoro-3-methoxypropanoic acid (PFMOPrA ; among PFECA alternatives to historical PFAS) to around -225 ppm for $-\text{CH}_2\text{F}$ groups of florfenicol (vet antibiotic). It implies strong experimental constraints to ensure that no signals of interest are missed.

Sensitivity

With a 1/2 spin, a high gyromagnetic ratio (94% of ^1H) and a 100% isotopic abundance, ^{19}F NMR is theoretically only slightly less sensitive than ^1H NMR. In addition, fluorine nuclei exhibit relaxation times similar to those of protons, with T_2/T_1 ratios for ^{19}F close to 1.0, allowing the efficient acquisition of free induction decays (FID). Long transverse spin-spin relaxation T_2 insures sharp signals, and gives access to homo- and heteronuclear J-coupling values.

This combination of high sensitivity, favourable relaxation properties, 100% natural abundance of the magnetically active fluorine-19 isotope and a total absence of natural background noise makes fluorine's overall sensitivity in practice better than that of the proton.

Chemical shift range, J-couplings

Likewise, the electron-rich nature of fluorine (surrounded by 9 electrons, instead of one for hydrogen) makes the fluorine spin, and its ^{19}F chemical shift, much more sensitive to the details of its local environment and the structure of the molecule. Therefore the range of fluorine chemical shifts is much more extended for fluorine than for hydrogen. ^{19}F resonances span 700 ppm, with over 200 ppm specific to fluorinated organic compounds, as detailed in W. R. Dolbier's Guide to Fluorine NMR for Organic Chemists⁶¹ and illustrated in Figure 4.

The combination of a large chemical shift dispersion and sharp signals, reduces signal overlap as compared to ^1H NMR, and enables spectral separation even on similar groups, such as the CF_2 groups of long perfluoro-saturated chains of PFAS compounds. Similarly, the large range of homo- and heteronuclear J-couplings⁶¹ is a source of structural information.

A drawback related to this wide spectral range is the fact that even in a moderate magnetic field, the complete range of possible ^{19}F signals cannot be easily covered in a single experiment. For instance, on the 600 MHz instrument used in this study, a 200 ppm range requires a spectral width of 113 kHz, too large to be analysed using standard procedures.

Specificity

One of the main strengths of the NMR technique is its high specificity as it only observes the signals from the studied atomic nuclei. Thus, a ^{19}F spectrum detects all the fluorine in a sample regardless of their chemical details but is blind to all

other elements (such as hydrogen and carbon). This is a strong advantage that allows the development of fully untargeted analyses. In addition, as most solvents do not contain fluorine, they will not interfere with the ^{19}F NMR signal, allowing the use of a broad variety of solvents. Thus, in contrast to ^1H NMR, fully deuterated solvents are not necessary, except for a small deuterium amount used to lock the spectrometer field.

Quantitativity

With proper experimental parameters, NMR allows direct quantitative measurements as the observed signals are proportional to the quantity of matter being analysed. The area under the peak (or integral) of the NMR signals is a direct determination of the molecular concentration in the solution, provided that the experimental parameters affecting accuracy and precision of the measure (e.g. delays, pulses, and acquisition time) have been carefully calibrated and optimized.

Minimal sample preparation

Liquid NMR applications benefit from minimal and rapid sample preparation, leading to reduced sample loss and a maintained integrity of the analytes. Even for complex matrices, a minimal filtration or a quick centrifugation after dissolution is sufficient to remove suspended undissolved matter without extensive processing. No necessary sample derivatization nor sample specific standard requirements make NMR really easy to operate. The use of disposable sample containers effectively prevents from cross-sample contamination. It can accommodate highly concentrated samples, so serial dilutions are not required, reducing the risk of systematic error. NMR stands out for its non-invasive nature as samples do not interact directly with the instrument and can be recovered for later operations. Additionally its high solvents compatibility is a real advantage for dissolution, allowing for greater flexibility in selecting solvents. This versatility is interesting when working with complex formulations, facilitating the breakdown and solubilization of challenging compounds.

In particular, Dimethyl Sulfoxide (DMSO) is often a preferred option due to its excellent solvating ability. This solvent dissolves both polar and nonpolar compounds, which makes it particularly useful for extracting varieties of compounds with favourable recovery rate, and especially suitable for effective soil sample treatments, even USEPA researchers have highlighted in 2023 degradation phenomenon with 3 HPFO-DA family samples over their DMSO screening stock of 205 PFAS, i.e. HPFO-DA, hexafluoropropylene oxide trimer acid (HFPO-TA) and tetramer acid (HFPO-TeA).⁶² In our experience, unless when HFPO-DA degrades, it forms a clean similar compound, likely Fluoroether E1, exhibiting a typical $-\text{CHF}_2$ signal, which should not alter the final quantification. Therefore, while DMSO is commonly used for its solubility benefits, it's always crucial to assess whether it's the most suitable choice for specific experiments and analytes.

Efficiency

NMR offers a comprehensive approach to quantitative and untargeted analysis while standing out for its non-invasive nature, minimal sample preparation requirements, single calibration point, low matrix interference.

Most fluorine detection methods are based either on the fluoride ion alone or on fluorinated organic molecules only. ^{19}F NMR allows the observation of both forms by solution

NMR, provided ionic forms are soluble. In addition, insoluble forms can be analysed by solid-state NMR. The nature of inorganic fluoride species found in the environment largely depends on soil composition and environmental conditions such as pH, temperature, and moisture levels, making their solubility difficult to predict. Even when soluble, they differ from the characteristic PFAS NMR fingerprint, which allows clear distinction between these species.

As there is hardly any other fluorinated organic compounds in the wild apart from the manufactured ones, the presence of a signal in the NMR spectrum is almost always the signature of some non-natural molecules.

Indeed, unlike other analytical techniques, ^{19}F NMR will be able to detect all soluble fluorinated species present in the studied sample offering promising perspectives in the diagnosis of fluorinated pollutants even some sensitivity issues are expected and further identification challenges (Figure 3).

In the two last decades ^{19}F NMR spectroscopy has gained recognition⁶³ in investigation of the conformations, dynamics and interactions of biomacromolecules,^{64; 65; 66} ligand-based NMR screening for drug discovery,^{67; 68} structure determination of organic fluorine compounds,⁵⁸ quality control^{69; 70} and for environmental measurements of total PFAS⁷¹ and especially recently with Camdzic^{72; 73} or Gauthier.^{74; 75} This study aims to present further investigation and efforts to highlight the potential of ^{19}F NMR using broadband acquisition and advocate it as a complementary routine analytical strategy for obtaining additional information alongside existing methods.

3 Optimisation & improvement in ^{19}F qNMR measurements

3.1 Large spectral range

The wide range of chemical shifts of ^{19}F signals creates two difficulties: unbiased excitation and faithful detection of all the resonances, both make it difficult to insure reliable quantitative measurements, in particular at high magnetic fields.

The major difficulty is to insure a correct excitation of a wide spectral width. It is well known that a square excitation pulse results in a limited excitation bandwidth, which is inversely proportional to its duration. Amplitude and phase distortions arise due to off-resonance effects,^{76; 77} becoming more pronounced as the signal deviates further from the pulse carrier. As a result, only the center of the excitation window can be used reliably. For instance, as a rule of thumb for quantitative measurements, a pulse of 15 μsec is considered to only faithfully excite a 25 to 50 kHz region centered on the pulse carrier, which is far from being sufficient for our purpose. Several solutions are known to circumvent this difficulty,^{78; 79; 80; 81; 82} but present deficiencies in the presence of fast decaying signals or large J-couplings, due to their long duration.

In order to address these issues we chose to use the OPERA pulse approach (Optimizing Phase of Excitation Removes Artifacts), a recent broadband excitation scheme presented by Coote *et al.*⁸³ (see Figure 5A). It has been designed using optimal control theory to reduce pulse duration while insuring no second order phase correction as observed with standard chirp pulses. The pulse has been optimized for several flip angles, and we chose to use the 45 degrees pulse definition

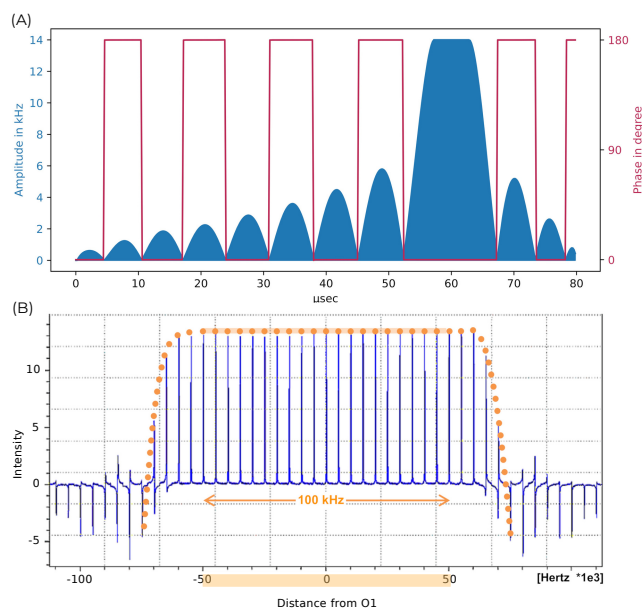


Figure 5. (A) OPERA-45 pulse shape designed by Coote *et al.*. Amplitude (in blue) and phase (in crimson) profile of the excitation waveform (pulse duration of 80 μs with RF amplitude of 14 kHz); (B) Experimental excitation profile measured by moving the carrier frequency of the OPERA-45 pulse on a 1 mM PFOA sample in DMSO-d6 under optimized conditions. The $-\text{CF}_3$ NMR signal intensity is consistent across a 120 kHz range of frequencies, meaning the excitation is uniform throughout the spectrum range.

which seems well adapted to quantitative studies. After phase correction, the flat excitation profile and the flat baseline permits reliable quantitative measurements (see Figure 5).

Experimental data on the OPERA-45 excitation pulse show a high-fidelity excitation over a 120 kHz bandwidth and robustness to power miss-calibration over 100 kHz (presented in the Supporting Information 1). In addition, the short duration of the OPERA-45 pulse (80 μsec) can suppress J-modulation artifacts for compounds with significant F-F coupling such as long chain PFAS compounds.

These features make it possible, through a one-shot experiment, to access the whole chemical information that would otherwise remain difficult to observe, as exemplified with a model compound in Figure 6. The single molecule Vertrel™ exhibits a chemical shift dispersion extending to 146.7 ppm. Moreover a reliable quantitation is achievable on this range, the uniform excitation of OPERA-45 ensuring that all integrated peaks in the spectrum are accurate and reliable.

In addition, on most spectrometers there is a marked loss of detection quality associated with the high sampling rates required for detection of large spectral widths, and on our 600 MHz instrument, this happens for widths larger than 100 kHz. This corresponds to a 177 ppm range, and implies that at least two acquisitions have to be made to cover the whole range of 200 ppm for possible organic fluorine signals. Instead, we decided to select a single region spanning from -50 ppm to -227 ppm, covering most of the possible signals, and to resort to additional measurements when needed.

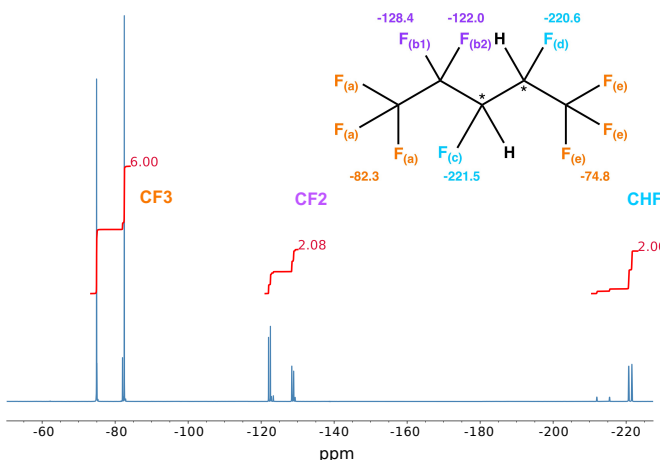


Figure 6. Broadband ^{19}F acquisition using OPERA-45 excitation, on 2H,3H-decafluoropentane 180 mM in DMSO-d6 (VertrelTM, technical grade, used as a zero ozone-depletion alternative to hydro chlorofluorocarbons). Primary and secondary alkyl fluorides exhibit significantly different shielding along the carbon backbone showing a chemical shifts dispersion of 146.7 ppm from $-\text{CF}_3$ moiety at -74.8 ppm to $-\text{CHF}_-$ groups around -221.5 ppm. With 2 chiral centers, and the CF₂ diastereotopic fluorines, NMR spectrum shows two distinct resonances profiles whose separation reflects proportion of some Vertrel stereoisomers. Acquisition in a single shot in quantitative conditions. Attributions are made using to ^{19}F - ^{13}C HMQC experiment in Figure 8.

3.2 2D experiments

Implementing two-dimensional NMR experiments is an important advantage for the characterization of unknown detected molecules.^{84, 85} Moreover, detecting fluorinated carbons in ^{13}C spectra can be challenging, especially when the signal-to-noise ratio is low, as their signals are spread across multiple lines and may blend into background noise. Figure 7 presents ^{13}C spectrum of our model compound (2H,3H-decafluoropentane, VertrelTM) revealing complex overlapping multiplets. An interesting approach could be to perform a ^{19}F - ^{13}C HMQC experiment with ^{19}F - ^{19}F decoupling (see below, OPERA-HMQC paragraph).

2D NMR can reveal signals that overlap in 1D NMR spectroscopy because of similar resonant frequencies and is indicative of mutually interacting spatial arrangements. A suite of NMR 2D ^{19}F - ^{19}F and ^{19}F - ^{13}C correlation experiments was implemented in the goal of providing a variety of experiments that will help interpret the spectra and elucidate the structure of the carbon backbone. The collected ^{19}F chemical shifts, along with the J_{HF} and J_{CF} coupling constants provide a wealth of information as exemplified in Figure 8. With the instrument generation that we use, the $\frac{\pi}{2}$ version of the OPERA pulse cannot be implemented because of too stringent timing constraints. As a consequence, we had to explore the possibilities left when using only the OPERA-45 version. With the main concern of PFAS pollution studies, in particular the identification of involved pollutants, we decided to principally implement the following 2D-experiments: ^{19}F - ^{13}C correlation, ^{19}F - ^{19}F correlation and ^{19}F DOSY.

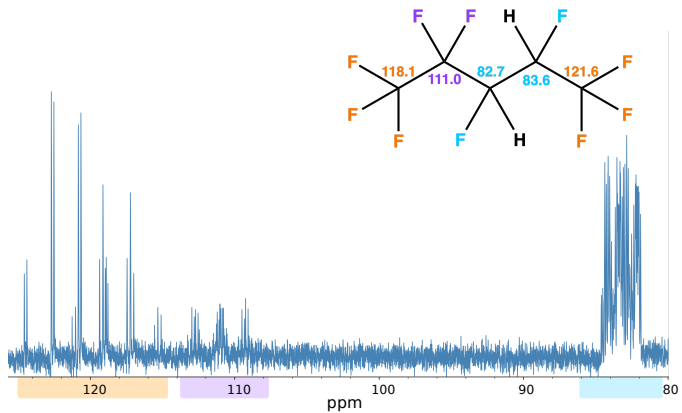


Figure 7. ^{13}C spectra of 2H,3H-decafluoropentane 180 mM in DMSO-d6 (VertrelTM). Fluorinated carbons in ^{13}C spectra can be difficult to assign, particularly due to J-couplings, their signals spread across multiple lines and may even merge with background noise. Assignment was made from the HMQC experiment.

OPERA-HMQC

The ^{19}F - ^{13}C 2D-correlation was implemented on the basis of the SOFAST HMQC (Selective Optimized Flip Angle Short Transient Heteronuclear Multiple Quantum Correlation)⁸⁶ experience because of its high sensitivity and restrained number of $\frac{\pi}{2}$ ^{19}F pulses resulting in shorter experimental time compared to conventional HSQC. ^{19}F π pulses were implemented using the CHIRP technique (Frequency-modulated pulse, see Supporting Information 2).⁷⁹

For our model compound the spectrum obtained is shown in Figure 8. Cross peaks show the various couplings along the backbone of the carbon chain. Both $^1\text{J}_{\text{CF}}$ and $^2\text{J}_{\text{CF}}$ coupling are observed. As expected, a carbon attached fluorine is characterized with a large ^{19}F - ^{13}C ^1J -coupling from 194 Hz to 281 Hz. HMQC enables clear distinction between the two methyl groups by examining two-bond coupling cross-peaks, aiding in the structural assignment of the molecule's various moieties

OPERA-COSY 45

The pulsed field gradient-enhanced COSY 45⁸⁷ was naturally used to implement ^{19}F - ^{19}F correlation enabling fast data collection while improving sensitivity and resolution (Frequency-modulated pulse, see Supporting Information 4). COSY 45 present the advantage of useful cross-correlation patterns to identify and interpret the interactions between fluorines within a molecule and to decipher multiple long range correlations, notably in PFAS (illustrated in Supporting Information 5 with PFOA). It is straightforward to implement and to use, with no modification to the standard sequence but the replacement of both pulses with OPERA-45, and works as expected.

Geminal homonuclear ^{19}F - ^{19}F J-coupling constants are very large (here 288 Hz), but even though the coupling constants diminish very quickly with the number of bonds, long-range J-couplings through even up to 5 bonds (^2J , ^3J , ^4J or ^5J) are not uncommon, as shown in Figure 9 in our model compound. For this reason, we used an additional delay τ in the ^{19}F -COSY in order to tune the range of detected J-values.

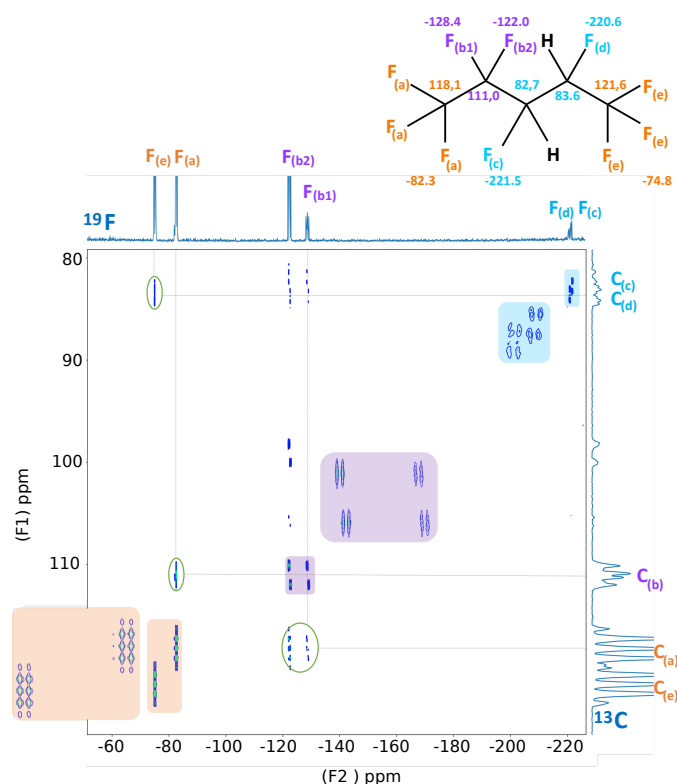


Figure 8. Broadband ^{19}F - ^{13}C HMQC on 2H,3H-decafluoropentane 180 mM in DMSO-d6 (VervetTM). Coupling patterns are enlarged for $^1\text{J}_{\text{CF}}$ coupling. This type of coupling is relatively strong for fluorine-carbon bonds, making it detectable and allow to confirm connectivity. $^1\text{J}_{\text{CF}}$ couplings were extracted from the F2-dimension: $^1\text{J}_{\text{CF}_a} = 281$ Hz, $^1\text{J}_{\text{CF}_e} = 281$ Hz, $^1\text{J}_{\text{CF}_{b1}} = 273$ Hz, $^1\text{J}_{\text{CF}_{b2}} = 255$ Hz, $^1\text{J}_{\text{CF}_c} = 203$ Hz, $^1\text{J}_{\text{CF}_d} = 194$ Hz. HMQC allows precise differentiation of the two methyl groups when we consider two-bond coupling cross-peaks circled in green between the fluorine nucleus $\text{F}_{(a)}$ at -82.3 ppm and the carbon nucleus $\text{C}_{(b)}$ at 111.0 ppm, between the fluorine nucleus $\text{F}_{(e)}$ at -74.8 ppm and the carbon nucleus $\text{C}_{(d)}$ at 83.6 ppm, and between the fluorine nucleus $\text{F}_{(b)}$ around -125 ppm and the carbon nucleus $\text{C}_{(a)}$ at 118.1 ppm. Artefact cross-peak around 100 ppm.

OPERA-DOSY

The ^{19}F DOSY experiment was implemented with the standard longitudinal eddy delay (LED) experiment^{88; 89} which does not require the use on π pulses (see Supporting Information 6). The set-up where only the final excitation pulse is implemented as an OPERA pulse was found to be the most sensitive.

3.3 Quantitative measure

As mentioned above, a reliable quantitative experiment requires properly tuned experimental parameters. To this end, we measured the T1 relaxation values of the PFOA molecule in 10% deuterated DMSO using both the saturation recovery and inversion recovery (IR) approaches (available in Supporting Information 8 and 9). The resulting values range from 0.35 to 0.86 s, the slowest relaxation time being found for the terminal $-\text{CF}_3$ moiety and the $-\text{CF}_2$ moiety located alpha to the functional group experiences faster longitudinal relaxation T1 at 0.35 s.

When adding scans in a repetitive acquisition, saturation due to the excitation pulse reduces the intensity of the signal,

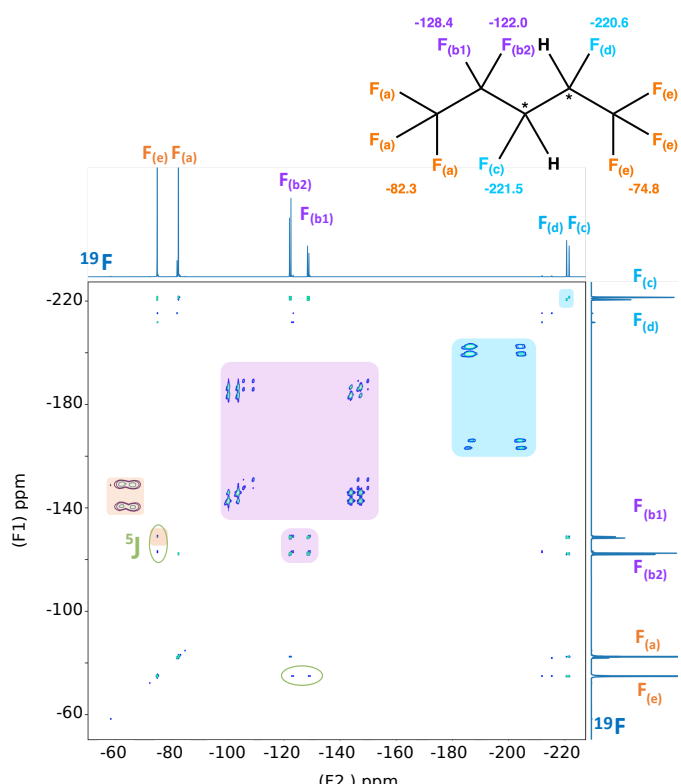


Figure 9. Broadband ^{19}F - ^{19}F COSY 45 on 2H,3H-decafluoropentane 180 mM in DMSO-d6 (VervetTM). Coupling patterns are enlarged. Purple zoom is showing the major and minor forms of this compound with two chiral centres. Long-range ^{19}F - ^{19}F J-couplings occur over multiple bonds. While vicinal (^3J) and geminal (^2J) couplings are most common, long-range couplings extend over five bonds (^5J).

and T1 relaxation imposes a minimal experimental repetition rate to recover a faithful intensity.

This minimum repetition time depends on the T1 value and also on the excitation flip angle.⁹⁰ For instance, with a $\frac{\pi}{2}$ flip angle, it is well known that a recovery time of at least 5 times the T1 value is required to achieve an accuracy of 99%, to the price of a lower signal sensitivity, while the same accuracy is obtained with a recovery time of only $3.5 \times \text{T1}$ with a 45° flip angle (see Supporting Information 10 for this relationship detailed).

Here, for routine quantitation using OPERA-45, we chose an accuracy of 97.5% corresponding to $2.5 \times \text{T1}$. Therefore, we set a relaxation delay of 1.5 s combined with an acquisition time of 0.66 s for a total repetition time of 2.16 s, these parameters allowing still a good sensitivity and a worst case accuracy of 97.5% for PFOA $-\text{CF}_3$ moiety.

3.4 Expressing qNMR results in mass equivalent of PFOA

The quantitative NMR signal is proportional to the molar concentration of the detected species in the sample. NMR reporting is based on molar quantities which are meaningful and consistent for comparisons of substance amounts, irrespective of their chemical nature. However, in environmental and pollution contexts, the mass ratio is the standard approach. Since NMR is an untargeted method, it enables the universal,

non-specific detection of all soluble fluorinated organic species in a given sample. This includes mono-fluorinated compounds, polyfluorinated molecules, soluble polymers, and PFAS—without requiring prior knowledge of the compounds or their molecular classification. However, without detailed knowledge of the molecular composition, it is difficult to trace back to the mass. Although ^{19}F NMR spectra can provide insights into the molecular family of fluorinated compounds, this information alone is insufficient for estimating molecular mass. Factors such as partial oligomerisation, non-fluorinated substituents (e.g., ester groups or heteroatoms), or variations in fatty chain length significantly affect molecular mass without altering the NMR signal, apart from minor, non-predictable chemical shift changes.

Given these complexities, we propose in this work three distinct approaches for reporting qNMR results, depending on the sample type and research focus:

Known Compounds or Characteristic Signals

When the detected compound is pre-identified or has a unique signal (e.g., trifluoroacetic acid), its molecular mass is known. This allows the weight ratio of the species to be directly calculated.

Class-Specific Analysis

For real-world samples when a specific class of compound is observed, the detected signal can be attributed to a representative compound from this class and expressed as an equivalent of this compound using with its molecular mass, representative for the entire class. For instance, when analysing PFAS, the detected signal can be expressed as an equivalent of a PFOA or PFOS, two well-characterised compounds with a molecular mass representative of the general PFAS family. For example, this approach assumes that the overall signal corresponds entirely to PFOA, thus yielding a content of PFAS in "PFOA mass equivalents".

Total Fluorine Concentration

Since all molecular fluorine in the sample generates an NMR signal directly proportional to its atomic molar concentration, the total amount of fluorine can be expressed as both molar concentration and fluorine weight ratio. This provides the total soluble fluorine content in the sample.

By employing these complementary approaches, qNMR results can be reported effectively across diverse analytical contexts.

4 Materials and methods

4.1 Materials and sample preparation

We have implemented the strategy outlined above on various scenarios, first with soil and water samples collected nearby an industrial plant producing PFAS containing materials, then with everyday life products either containing fluorinated ingredients or found to be contaminated.

Samples sourcing

Contaminated test samples, 3 soil samples (samples S1 to S3) and 3 water samples from adjacent river (samples W1 to W5), were provided by the French Agency for Food, Environmental and Occupational Health & Safety - ANSES's Nancy Laboratory. They were collected by ANSES from an industrial plant manufacturing products containing

PFAS. Location, finished product details, volume productions and ingredient use rates are unknown. A sample of the manufactured product (referred to as sample R) was also provided.

Pharmaceutical ingredients exemplified in this article were directly extracted from commercial tablets, capsules or spray medicines. Some daily life products were investigated and commercially purchased.

2H,3H-perfluoropentane [138495-42-8], also known as Vertrel™ was purchased from Scientific Alfa Aesar as technical grade 90%. Perfluorooctanoic acid PFOA 95% [335-67-1], 1H,1H,2H,2H-Perfluorooctanol FTOH 97% [647-42-7], Perfluorodecanoic acid PFDA 97% [335-76-2], Perfluorotetradecanoic acid PFTeDA 96% [376-06-7] were also sourced from Scientific Alfa Aesar. Perfluorooctanesulfonic acid potassium salt PFOS 98% [2795-39-3], Perfluoro-3,6-dioxadecanoic acid PFO₂DA [137780-69-9], Perfluoro-3,6,9-trioxatridecanoic acid PFO₃TDA [330562-41-9], 1H,1H,2H,2H-Tridecafluoroctane-1-sulphonic acid 6:2 FTSA [27619-97-2] were obtained from Sigma Aldrich. Perfluoro(2-methyl-3-oxahexanoic) acid GenX [13252-13-6] was acquired from Manchester Organics, Perfluoro(2-methylpentan-3-one) [756-13-8] from Apollo Scientific Ltd and Perfluoro-3-methoxypropanoic acid PFMOPrA [377-73-1] from Enamine. No additional purification and fractionation were performed.

All solutions for NMR measurements were prepared using a homemade solution of 10% DMSO-d6 in DMSO. Deuterated solvents (DMSO-d6, D₂O) were acquired from Eurisotop and DMSO from Sigma Aldrich.

Samples preparation

• Pharmaceutical sample references

To extract some active ingredient from commercial tablets, capsules, etc. the sample was grinded into a fine powder, poured into DMSO - DMSO-d6 9:1(v/v), shaken for a few minutes and allowed to sit. Supernatant was collected and directly introduced into a 5 mm NMR tube for reference.

• Polluted water samples from industrial plant

The liquid samples are studied directly in 5 mm NMR tubes with 500 μL of sample and 100 μL of D₂O.

• Polluted soil samples from industrial plant

An exact mass around 50 milligrams of soil (air-dried and sieved) was macerated for 12 h at room temperature in a mixture of DMSO - DMSO-d6 9:1(v/v) according to a weight/volume ratio of 20%. After centrifugation, the supernatant was collected and directly introduced into a 5 mm NMR tube.

• Liquid samples

All liquid samples were studied directly in 5 mm NMR tubes with 540 μL of sample and 60 μL of DMSO-d6.

• Cosmetics or oral hygiene care samples

To extract creamy foundation product, concealer, powder eye shadow or toothpaste, the material was poured into DMSO - DMSO-d6 9:1(v/v), shaken for a few minutes and allowed to sit. Supernatant was collected and directly introduced into a 5 mm NMR tube.

4.2 NMR analysis

^{19}F spectra were acquired on a Bruker spectrometer 600 MHz Avance I (Bruker BioSpin, Rheinstetten, Germany) equipped with a Quadruple Resonance CryoProbe 5 mm QCI-F allowing sensitivity increase by a factor of three on ^{19}F . They were collected operating at the ^{19}F resonance frequency of 564.607990 MHz at 298 K under the control of Topspin-2.1 (Bruker BioSpin). ^{19}F referencing was performed according the IUPAC convention⁹¹ with no need of a fluorinated reference material. The inversion recovery pulse sequence was used for longitudinal relaxation time (T1) determination, and a python program used to extract the values, using a standard least-square 3 parameters approach (see Supporting Information 9).

1D experiments

The 1D ^{19}F qNMR experiments were recorded using OPERA-45 shaped pulse.⁸³ They were acquired with a 100 kHz spectral width (177.11 ppm), with the digital filtering set to smooth, on 128 k points (0.65 s acquisition time) and a 1.5 s relaxation delay. Experiments were acquired using block strategy, where the data were stored independently every 256 scans, and co-added during the Fourier processing. The number of blocks was adapted for each sample according to the required signal-to-noise ratio.

All 1D experiments were processed as follows: the FID was apodized with a 30 Hz wide Gaussian broadening, zero-filled twice before Fourier transform, and phase corrected. When needed, to correct for baseline distortion, the spectrum was reverse Fourier transformed and the 8 first points of the reconstructed FID corrected by a reverse Linear Prediction computation using the fast Burg algorithm and Fourier transformed back. The baseline was further optimized by applying a spline correction computed from the empty region of the spectrum.

Quantification was performed by integration of the specific line in the spectrum. Quantification results are computed from the area under the curve as molar concentration by correcting for the effective number of scans (related to the number of blocks) and expressed in weight ratio with respect of the original sample. Unknown compounds are expressed as PFOA equivalent (see 3.4 Expressing qNMR results in mass equivalent of PFOA).

2D experiments

The HMQC experiment was performed using the SoFast-HMQC sequence (presented in the Supporting Information 2). The 2H,3H-decafluoropentane (Vertrel™) sample was at a concentration of 180 mM in d6-DMSO. Each FID was acquired with a 100 kHz spectral width (177.11 ppm), with the Digital filtering set to smooth, on 4 k points and with a 1.94 s relaxation delay. The ^{19}F excitation pulse was the same OPERA-45 pulse as used in other experiments. The ^{19}F refocusing pulse as well as the initial inversion SoFast pulse were performed using a 1.5 ms chirp pulse, covering a 300 kHz frequency range, with a B1 power at 6.18 kHz. The ^{13}C $\frac{\pi}{2}$ pulses were 20 μs . Four scans were acquired per increment and 1024 increments were performed for a total acquisition time of 2 hours 15 min.

The COSY-45 experiment was acquired using a modified sequence, using ^1H decoupling (see Supporting Information 4).

Both HMQC and COSY experiments were apodized with

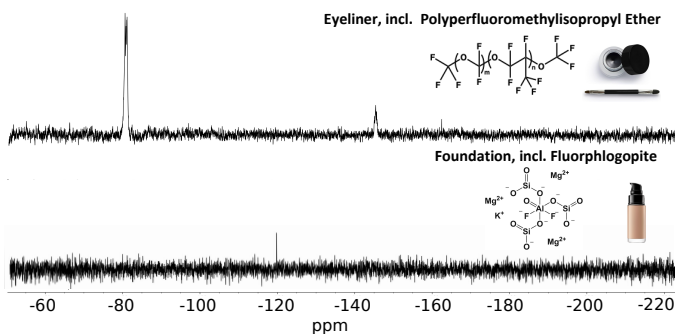


Figure 10. ^{19}F NMR spectra of two cosmetic products. (1) A foundation with synthetic fluorphlogopite additive used to add a glittering effect to products, giving rise to a peak at -119.1 ppm; (2) An eyeliner with polyperfluoromethylisopropyl ether polymer to make it longer lasting and water-proof, giving rise to 3 patterns around -59 ppm, a really weakly distinguishable signal for terminal $-\text{OCF}_3$, at -80.5 ppm for the $-\text{OCF}_2$ - and $-\text{CF}_3$ - polymeric moieties and at -145.1 ppm for $-\text{CF}$ - polymeric moieties.

shifted sine-bell along both dimensions, zero-filled once on each axis, and computed in magnitude after FT. All the DOSY experiments were computed using the PALMA algorithm⁹².

All NMR spectra were processed using an open-source Python package dedicated to Fourier spectroscopies called "Spectrometry Processing Innovative KErnel" (SPIKE).⁹³ All data series were processed with a automatic pipeline program derived from Plasmodesma, an autonomous unsupervised processing of set of 1D and 2D NMR experiments which guarantees homogeneous data processing within the set.^{94; 95}

5 Results Case studies

5.1 Detection with daily life products

We have tested the procedure presented above on some everyday products including food, cosmetics and hygiene products, pharmaceuticals and agrochemicals. The products included various common items, representing a range of chemical compositions from fluorinated compounds, perfluorinated substances to fluoride species. We exemplified with some NMR profiles highlighting typical encountered situations, either products containing fluorinated ingredients or found to be contaminated. However in this case we are unable to determine whether contaminants are due to poor manufacturing practices, packaging pollution or to the use of polluted raw materials.

Claimed fluorinated ingredients

In Figure 10, we present spectra of cosmetic products containing fluorinated ingredients, as identified in their official ingredient lists: synthetic fluorphlogopite and polyperfluoromethylisopropyl ether polymer. Until recently, PFAS were used in cosmetics for their ability to make products long-lasting, water-resistant, and smudge-proof as well as for product consistency, texture and longevity issues. The most common used were polytetrafluoroethylene (PTFE) and perfluorodecalin, along with perfluorooctyl triethoxysilane, perfluorononyl dimethicone or perfluorohexane. The manufacture and use of fluorine-containing cosmetics

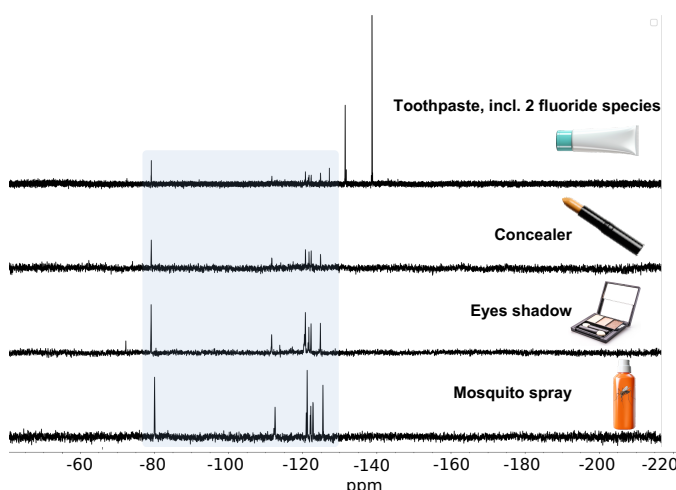


Figure 11. ^{19}F NMR spectra of four PFAS contaminated samples from commercial daily life products (toothpaste, concealer, eye shadow and mosquito repellent spray) exhibiting the characteristic PFAS fingerprint grouping three sets of signals around -80, -115 ppm and a last cluster centred around -123 ppm (highlighted in blue).

not only pose health risks but contribute to environmental pollution particularly through washing off and, ultimately, disposal.

Tested cosmetics include a foundation with fluorophlogopite, a synthetic mica also used in nail polish, eye shadow or lip gloss; and an eyeliner formulated with a polyperfluoromethylisopropyl ether additive. This last compound, introduced as one of the first fluorinated polymers for cosmetics since the late 1980s, is recognized for enhancing waterproof performance.

Some toothpaste samples have been explored. It is one of the most commonly used healthcare products. Various fluoride additives are incorporated in commercial toothpaste formulations to prevent tooth decay; among them sodium fluoride (NaF), sodium monofluorophosphate ($\text{Na}_2\text{PO}_3\text{F}$), stannous fluoride (SnF_2) or Olaflur, an alkyl-ammonium fluoride. Regardless of the fluorine compound or the toothpaste formulation, claimed fluorine ingredients can be visualized by ^{19}F NMR (see Supporting Information 11).

The ^{19}F NMR technique enables also the precise observation of the active substance in fluorine-based medicine while also ensuring the detection or confirmation of the absence of other potential fluorine-based impurities. This approach is useful for quality control,⁶⁹ guaranteeing the purity and efficacy of pharmaceutical formulations (see Supporting Information 12).

PFAS contaminations

In parallel, contamination of cosmetics with PFAS is becoming a growing issue in recent years,⁹⁶ since cosmetics applied to the skin, face, and hair can be a potential route of exposure to harmful chemicals, leading to various health risks over time. PFAS were initially added to cosmetics to provide smoothness and shine, while also improving the product's texture. In some cases, they can also incidentally appear in cosmetics due to impurities in raw materials or packaging issues. PFAS-like

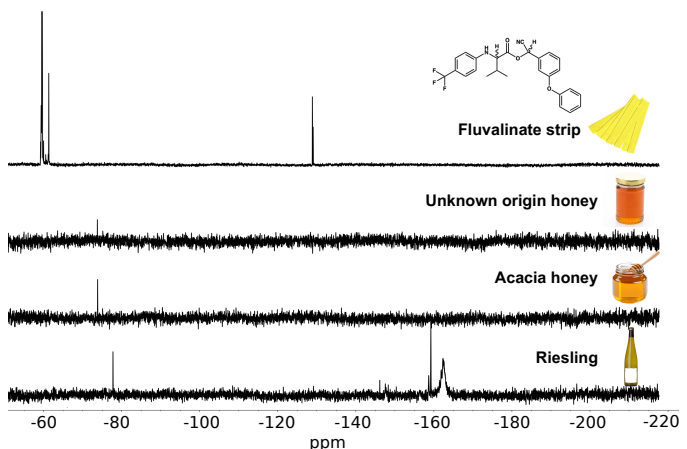


Figure 12. ^{19}F NMR spectra of four consumer market products with fluorinated contaminants. (1) Riesling sample displaying multiple peaks: singlet at -77.7, -146.0, -150.2, -158.5 and -159.1 and two complex patterns around -147.6 and -162.2 ppm. (2-3) Both honey from different sources exhibiting peak at -73.7 ppm. (4) Hive treatment product supposed to contain fluvalinate corresponding to the peak around -59.5 ppm but containing at least another fluorinated substances with unexpected peaks at -61.3, -128.7 and -128.9 ppm.

impurities have been observed in a eye shadow powder and a concealer with their classical ^{19}F NMR fingerprints, combining three characteristic patterns two of them around -80, -115 ppm and a last cluster centred around -123 ppm. Likewise among tested hygienic products, a mosquito repellent in spray and a toothpaste were found to contain PFAS. Again we are unable to determine whether contaminants are due to poor manufacturing practices, packaging pollution or to the use of polluted raw materials (see Figure 11).

Fluorinated contaminations

We also disclose the spectrum of an acaricide strip based on fluvalinate, marketed for honey bee protection. The spectrum reveals a characteristic peak around -60 ppm, indicative of its primary active component isomers, along with additional unexpected peaks at -61.3, -128.7 and -128.9 ppm, potentially associated with at least another fluorinated compound not mentioned in claimed composition. Impurities that may originate from various sources, such as synthesis residues, formulation, or packaging, like active substances, will end up in the environment.

While the likelihood of fluorinated compounds being present in wine should be generally low due to controlled agricultural practices, concerns might even arise from vineyard contamination, packaging materials leaks or an industrial proximity. Traces of fluorinated compounds in a French Alsatian white wine, from Riesling grape were found.

Similarly, two of six honey samples (first-price honey without specified provenance, and an acacia honey) also showed traces with a single peak at -73.8 ppm as shown in Figure 12

Manufacture of PFAS containing material

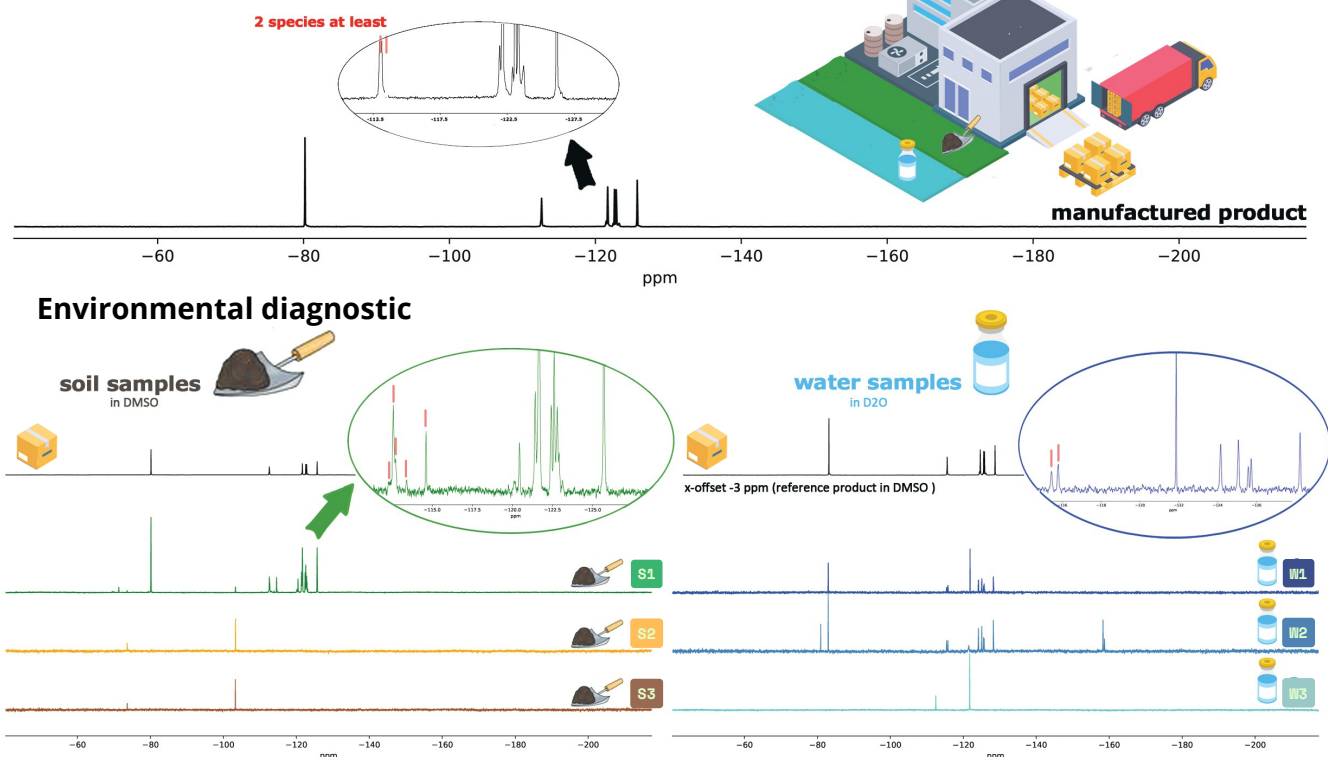


Figure 13. Diagnosis of PFAS pollution nearby an industrial plant manufacturing PFAS containing material. Three water samples (blue spectra) were collected from a nearby river, and three soil samples (green spectra) were taken from an adjoining plot. They were analysed by ^{19}F NMR and compared against the reference product (at least two species, one of which is very marginal according the right shoulder of the peak at -80.16 ppm). The manufactured product (black spectrum) exhibits the characteristic three-part PFAS fingerprint with signals at -80.16, -112.60 ppm and a last cluster centred around -123 ppm. This similar pattern was found in soil sample S1 and water samples W1 and W2. Soil sample S1 exhibits others peaks at -112.40, -112.75, -113.42 and -114.58 ppm revealing at least 4 others PFAS species. Minor peaks, observed nearby -71.0 -73.5 and -103.1 ppm, were neither identified nor correlated with each other. S2 and S3 show very similar NMR profiles without the classical three-part PFAS fingerprint. Both peaks at -73.5 and -103.1 ppm are also found in S2 and S3 soils. Water samples W1 and W2 contain at least two PFAS species with two peaks at -115.4 and -115.7 ppm, along with singlet at -82.9 ppm and cluster at -126.0 ppm, the characteristic pattern of PFAS. Additional peaks at -80.9, -121.5, -158.3 and -158.7 ppm were found in W2 revealing presence of more fluorinated compounds. The peak at -121.5 ppm appears also in W1 and W3 along with a singlet at -112.3 ppm.

5.2 Industrial plant pollution diagnosis

In case of suspected pollution, a comprehensive environmental monitoring of pollutants is necessary in order to track pollution source and levels as well as to carry out efficient remedial measures. We present here an investigation by ^{19}F NMR of the occurrence of fluorinated contaminants in soil and water samples gathered during an ANSES sampling campaign at an industrial contaminated site (Figure 13). To assess potential PFAS pollution in the vicinity of this industrial facility, environmental samples were compared against the reference PFAS-containing product known to be used or produced at the industrial plant. The analyses have been performed using the protocols described here and summarized in Table 1.

Reference PFAS-containing material sourced from the plant

Interestingly, we also obtained a reference product, either the intended manufactured product or ingredients used during the process, however the structure of which was not disclosed to us. Its ^{19}F NMR fingerprints, with a characteristic pattern

consisting in two signals around -80 and -112 ppm and last cluster centred around -123 ppm, is consistent with known PFAS structural motifs, and in particular fluorotelomer species. Indeed the chemical shift of $-\text{CF}_2$ group closest to the functional group can serve as a distinctive marker, at least enabling rapid spectral distinction between perfluorinated (PFCA, PFSA, PFPA, FASA) typically around -115 ppm in DMSO-d₆ or polyfluorinated (FTOH, FTSA, FTCA, N-alkyl FASA) which tend to appear closer to -112 ppm.

Qualitative analysis of environmental samples

The pattern of the reference PFAS-containing product was found in one soil sample S1 and two of the water samples W1 and W2, whereas S2, S3 and W3 didn't show this characteristic three-part PFAS fingerprint. Sample S1 exhibits several PFAS species (at least five), including two major ones, one that could be identified as a fluorotelomer and another as a perfluorinated compound according to their chemical shifts. Additional peaks reveal the presence of more fluorinated compounds in these samples. Nevertheless, whereas S2 and S3 exhibit highly

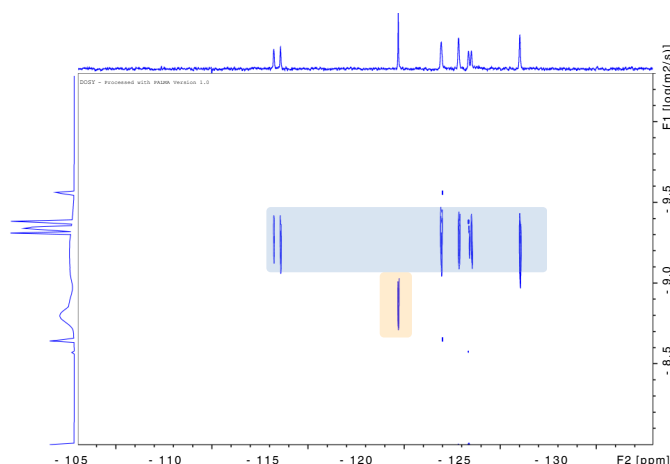


Figure 14. DOSY experiment on W1 sample. Two molecular populations with clearly differentiated coefficients of diffusion are highlighted.

similar NMR profiles with two well-separated peaks in the spectrum, they are only detectable with extended experiment durations indicating a minimal pollution. Two of the water samples (W1, W2) present the fingerprint of the manufactured material but show profiles slightly different from the S1 soil sample. They display different additional species. Sample W2 exhibits an unusual peak nearby -158 ppm, suggesting the presence of a compound with tertiary carbon-fluorine centre. DOSY experiments were performed on the W1 and the S1 samples in order to obtain additional information. It clearly reveals two distinct populations in W1 sample, one of which is PFAS-related and the other of a lighter species with a higher diffusion coefficient (Figure 14). S1 shows a greater complexity in the PFAS components, which suggest at least two different diffusion coefficients and thus two species, as previously suspected based on the $-\text{CF}_2-$ group alpha to the functional groups.

The PFAS contamination is most likely originated from production, as characteristic NMR fingerprints of the manufactured material were directly found in one soil sample and 2 water samples.

Quantitative analysis of environmental samples

While individual substances cannot be fully identified from this single experiment —nor was that the objective— it remains possible to quantify the total PFAS content using an external PFOA reference calibration.

Regarding the signal of interest, we found that in case of complex polluted mixture or samples integrating PFECA type molecules, the $-\text{CF}_2-$ moiety located alpha to the functional group is most significant because of reduced overlap with other spectral features. The $-\text{CF}_3$ region may include additional contributions from overlapping $-\text{CF}_2\text{O}-$ moieties.

The intensity of the NMR signal is characteristic to the number of molecules rather than to their mass, for this reason the results are naturally presented here in molar concentration of the analyte in the analysed matrices. The T1 table presents the quantification results.

The most loaded sample, S1, was found to contain 753

Table 1. Quantification results

Sample	[PFAS _{total}]	[F _{total}]
S1	753 nmol/g	6000 nmol/g
S2	<LOD	67 nmol/g
S3	<LOD	57 nmol/g
W1	48 μM	390 μM
W2	13 μM	137 μM
W3	<LOD	22 μM

nmol PFAS per gramme of dry soil after a 12-hours extraction, as 3 hours was insufficient for a complete extraction.

For comparative purposes to others methods, we also propose to express this content in terms of mass as PFOA equivalents (see section 3.4), a way of assuming "artificially" that all $-\text{CF}_2-$ signals adjacent to the terminal functionality are due to PFOA, an approach which is coherent as all CF_2 have the same molar mass. Thus using the molar mass of PFOA (MW=414.07 g/mol) as the average molar mass of the present chemical species, this soil is found highly contaminated at 312 $\mu\text{g PFOA}_{\text{equiv}}/\text{g dry soil}$.

The pollutants in soil samples S2 and S3 were only detectable after an extended experiment duration, indicating they are much less polluted, with concentrations below the limit of detection (LOD) for PFAS within a reasonable time frame (4096 scans), even if around 60 nmol/g of fluorine were detected.

Occurrence of per- and polyfluoroalkyl substances (PFAS) in soil and water sample indicate an environmental pollution originating from the industrial plant, either impacted by industrial effluents or receiving run-off or deposition from the site. While PFAS are claimed to be "forever chemicals", they may be subject to possible chemical transformations upon deposition, which might account for the variations in the content and the concentrations observed in the different analysed samples.

6 Concluding remarks and outlook

Comprehensive diagnosis tool

The diagnosis workflow summarized in Figure 15 illustrates the use of ^{19}F NMR spectroscopy for quantifying soluble fluorine content in various samples as either total fluorine content or total PFAS content using their characteristic NMR fingerprints. The modification of active ingredients with fluorine or fluorinated motifs, remains an important method for designing efficient new chemical entities, because the fluorine atoms modulate the properties of active molecules as well as improving their sturdiness. Chemists have developed numerous and immensely diverse fluorinated compounds, which finally end up in the environment. We believe ^{19}F NMR offers a robust strategy to observe the whole scope of these fluorinated pollutants. Traditional targeted approaches often fail to capture the broader contamination landscape, leaving gaps in monitoring and remediation strategies. An untargeted diagnosis tool like ^{19}F NMR could act as a "hot-spot" indicator, identifying areas that warrant further investigation. It addresses the limitations of conventional techniques, which largely focus on specific, pre-characterized compounds and are unable to map the full extent of contamination. Or even more, a synergistic strategy integrating LC-MS/MS and NMR —an

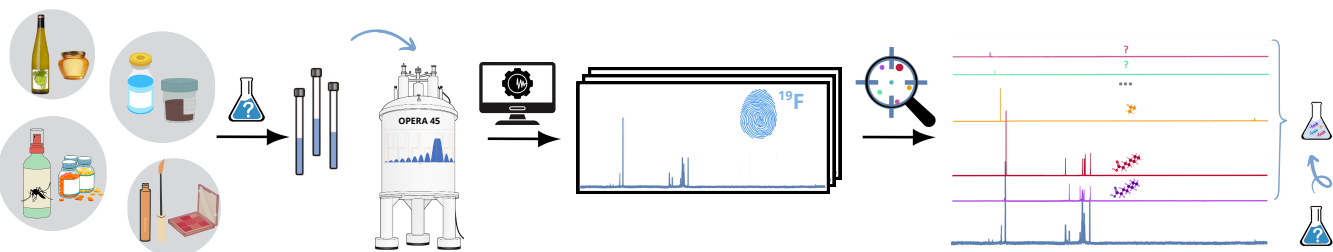


Figure 15. General workflow of fluorinated content diagnosis based on ^{19}F NMR acting as an universal detector. Various samples either soluble or extractable can investigated (cosmetic, food, medicine, environment...). qNMR can offer high-throughput analysis by offering simple minimalist sample preparation, while providing an unbiased overview of the whole soluble fluorine sample content. Credit NMR instrument: Wikimedia - Database Center for Life Science (DBCLS).

approach validated in omics research^{97, 98}—could provide a more robust analytical framework. Now more than ever, the iceberg analogy is crucial: targeted methods reveal only the tip of the problem, leaving the largest part hidden beneath the surface as shown in Figure 16.

Easy-to-handle diagnosis tool

Through a simple procedure of straightforward dilution or extraction followed by a spectrum acquisition, ^{19}F NMR provides a direct and thorough assessment of the total fluorinated content, without prior conversion of samples into instrument-compatible formats. The spectra directly reflect the presence of all fluorinated contaminants, PFAS or non-PFAS, expected or unexpected, native or degradation products, offering an untargeted approach to pollution analysis. The procedure developed here, based on the OPERA-45 sequence appears to be an elegant and efficient way to conduct fluorine pollution analysis by NMR and was applied to several analysis scenarios. The OPERA-45 pulse is reliable, robust and particularly suitable for large spectral widths and compounds exhibiting strong homonuclear J-coupling like PFAS. Although pre-concentration efforts may be necessary to address the sensitivity limitations of ^{19}F NMR in low concentration samples, handling procedures remain minimalist, ensuring an absence of cross pollution and the sample integrity.

Moderate to high level pollution diagnosis tool

As of today, using acquisition time in the order of hours, we experienced a Limit of Detection (LOD) around 500 nmol/L or 1.5 nmol/g for typical medium-sized molecules. For a small molecule as trifluoroacetic acid (TFA), the LOD can be as low as 150 nmol/L, which corresponds to roughly 20 $\mu\text{g}/\text{L}$ (ng/mL). Limit of Quantification (LOQ), typically defined as three times the LOD according to the signal-to-noise based definition, rises to low μM , around 5 nmol/g for solid samples or typically for TFA about 60 ng/mL.

For PFAS compounds, in terms of mass concentration, the Limit of Quantification (LOQ) would be in the order of 500 $\mu\text{g}/\text{L}$ in liquid matrices and 2.5 $\mu\text{g}/\text{g}$ in soil sample, eventually reconcentration would improve these figures. So the focus for NMR analysis is not in detecting trace amounts but rather in identifying and quantifying pollution at significant concentrations. This means that instead of working at trace levels as in mass spectrometry, NMR is better suited to the analysis of contamination at moderate to high levels, where larger quantities of pollutants are present in a

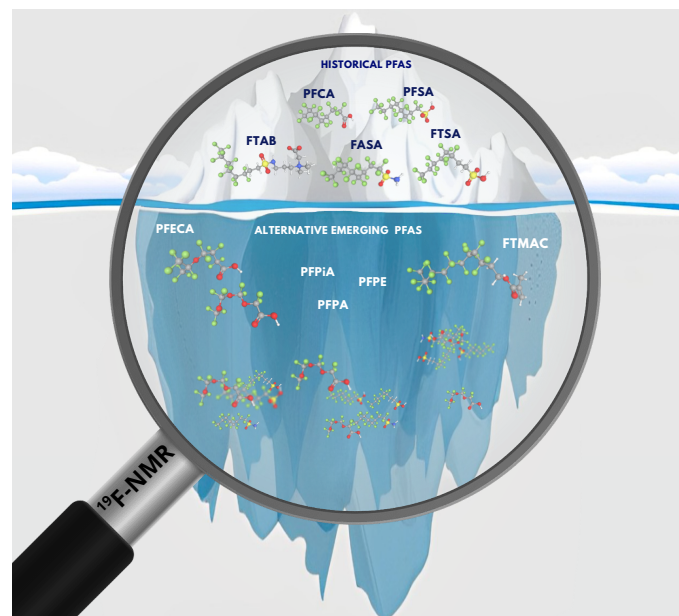


Figure 16. ^{19}F NMR as a complete tool for untargeted and impartial analysis, as targeted analysis only allows you to see the tip of the iceberg.

sample. Moreover, it can be expected that under continuous development of the NMR technologies in specific cryo-probes and higher fields, the sensitivity and resolution of the technique can still be extended.

As illustrated throughout this study, ^{19}F NMR offers a comprehensive strategy for observing the full range of fluorinated pollutants. From its ability to detect all soluble fluorine species this untargeted, unbiased approach method stands out as a promising solution for tackling the complexity of fluorine pollution. However, to realize its full potential, continuous innovation and optimization will be required to address practical challenges it faces, including sample preparation, sensitivity enhancement, and data interpretation to identify individual substances. We are confident that with further advancements, ^{19}F NMR will become an invaluable tool for monitoring fluorinated contaminants, contributing to environmental protection and public health efforts on a global scale.

Author contributions

M.A.D. conceived of the foundational idea. J.A.H. made the proof of concept. A.B.D. investigated, developed, and implemented the study, leading to the fully refined and completed concept. M.A.D implemented the presented NMR sequence and developed the original processing tool. A.B.D. performed almost all the acquisitions and carried out the experiments and the sample preparations. L.D. supported processing tools development to analyse data and helped some sample preparations and acquisition. A.B.D. wrote the manuscript with input of M.A.D and L.D. M.A.D. wrote the supporting information with input of A.B.D. and L.D.

Acknowledgments

We thank ANSES for providing test samples and the French National Agency for Research ANR for financial supporting under the grant number ANR-18-CE44-009.

Financial disclosure

None reported.

Conflict of interest

The authors declare no potential conflict of interests.

REFERENCES

- Dehnen S, Schafer LL, Lectka T, Togni A. , Fluorine: A Very Special Element and Its Very Special Impacts on Chemistry. *Org. Lett.* **2021**, *23*, 9013–9019. doi: [10.1021/acs.orglett.1c03799](https://doi.org/10.1021/acs.orglett.1c03799)
- Smart BE. , Fluorine substituent effects (on bioactivity). *J. Fluorine Chem.* **2001**, *109*, 3-11. doi: [10.1016/S0022-1139\(01\)00375-X](https://doi.org/10.1016/S0022-1139(01)00375-X)
- Solvay Products & Solutions, Organic Fluorinated Compounds-Raw materials, Intermediates & Active ingredients. <https://www.solvay.com/en/chemical-categories/fluorine-chemicals/organic-fluorinated-compounds> (accessed 4 April 2025); **2025**. Published online.
- Purser S, Moore PR, Swallow S, Gouverneur V. , Fluorine in medicinal chemistry. *Chem. Soc. Rev.* **2008**, *37*, 320-330. doi: [10.1039/B610213C](https://doi.org/10.1039/B610213C)
- Inoue M, Sumii Y, Shibata N. , Contribution of Organofluorine Compounds to Pharmaceuticals. *ACS Omega* **2020**, *5*, 10633-10640. doi: [10.1021/acsomega.0c00830](https://doi.org/10.1021/acsomega.0c00830)
- Shabir G, Saeed A, Zahid W, et al. , Chemistry and Pharmacology of Fluorinated Drugs Approved by the FDA (2016–2022). *Pharmaceuticals* **2023**, *16*, 1162-1212. doi: [10.3390/ph16081162](https://doi.org/10.3390/ph16081162)
- Henary E, Casa S, Dost TL, Sloop JC, Henary M. , The Role of Small Molecules Containing Fluorine Atoms in Medicine and Imaging Applications. *Pharmaceuticals* **2024**, *17*, 281-306. doi: [10.3390/ph17030281](https://doi.org/10.3390/ph17030281)
- Jeschke P. , The Unique Role of Fluorine in the Design of Active Ingredients for Modern Crop Protection. *ChemBioChem* **2004**, *5*, 570-589. doi: [10.1002/cbic.200300833](https://doi.org/10.1002/cbic.200300833)
- Ogawa Y, Tokunaga E, Kobayashi O, Hirai K, Shibata N. , Current Contributions of Organofluorine Compounds to the Agrochemical Industry. *iScience* **2020**, *23*, 101467. doi: [10.1016/j.isci.2020.101467](https://doi.org/10.1016/j.isci.2020.101467)
- Buck RC, Franklin J, Berger U, et al. , Perfluoroalkyl and polyfluoroalkyl substances in the environment: Terminology, classification, and origins. *Integrated Environmental Assessment and Management* **2011**, *7*, 513-541. doi: [10.1002/ieam.258](https://doi.org/10.1002/ieam.258)
- Sauvé S, Desrosiers M. , A review of what is an emerging contaminant. *Chem. Cent. J.* **2014**, *8*, 15. doi: [10.1186/1752-153X-8-15](https://doi.org/10.1186/1752-153X-8-15)
- Stockholm Convention, What are POPs?. <https://chm.pops.int/TheConvention/ThePOPs/tabid/673/Default.aspx> (accessed 4 April 2025); **2025**. Published online.
- Gaines LGT. , Historical and current usage of per- and polyfluoroalkyl substances (PFAS): A literature review. *Am. J. Ind. Med.* **2022**, *66*, 353–378. doi: [10.1002/ajim.23362](https://doi.org/10.1002/ajim.23362)
- Glüge J, Scheringer M, Cousins IT, et al. , An overview of the uses of per- and polyfluoroalkyl substances (PFAS). *Environ. Sci.: Process. Impacts* **2020**, *22*, 2345-2373. doi: [10.1039/D0EM00291G](https://doi.org/10.1039/D0EM00291G)
- Figuère R, Miaz LT, Savvidou E, Cousins IT. , An Overview of Potential Alternatives for the Multiple Uses of Per- and Polyfluoroalkyl Substances. *Environ. Sci. Technol.* **2025**, *59*, 2031-2042. doi: [10.1021/acs.est.4c09088](https://doi.org/10.1021/acs.est.4c09088)
- Plunkett RJ. , Oral History Interview, by Bohning, James J. on 1986-Apr-14 (First session) and 1986-May-27 (Second session). <https://digital.sciencehistory.org/works/0g354g32t#tab=ohDescription> (accessed 31 March 2025); **2025**. Published online.
- Ebnajesjad S. , Discovery and History of Fluoropolymers. In: *Introduction to Fluoropolymers*, , William Andrew Publishing, Oxford, **2013**, 17-35
- USEPA deems two GenX PFAS chemicals more toxic than PFOA. *Chem. Eng. News* **2021**, *99*. According to a USEPA assessment, October 2021. <https://www.epa.gov/chemical-research/human-health-toxicity-assessments-genx-chemicals> (accessed 4 April 2025).
- Xin Y, Ren XM, Wan B, Guo LH. , Comparative in Vitro and in Vivo Evaluation of the Estrogenic Effect of Hexafluoropropylene Oxide Homologues. *Environ. Sci. Technol.* **2019**, *53*, 8371-8380. doi: [10.1021/acs.est.9b01579](https://doi.org/10.1021/acs.est.9b01579)
- Mahoney H, Xie Y, Brinkmann M, Giesy JP. , Next generation per- and poly-fluoroalkyl substances: Status and trends, aquatic toxicity, and risk assessment. *Eco-Environment & Health* **2022**, *1*, 117-131. doi: [10.1016/j.eehl.2022.05.002](https://doi.org/10.1016/j.eehl.2022.05.002)
- Evich MG, Davis MJB, McCord JP, et al. , Per- and polyfluoroalkyl substances in the environment. *Science* **2022**, *375*. doi: [10.1126/science.abg9065](https://doi.org/10.1126/science.abg9065)
- European Chemicals Agency publishes PFAS restriction proposal. <https://echa.europa.eu/fr/-/echa-publishes-pfas-restriction-proposal> (accessed 4 April 2025); **2025**. Published online.
- United States Environmental Protection Agency, CompTox Chemicals Dashboard v2.4.1, Contaminant Candidate List CCL 5 PFAS subset: 10.246 chemicals. <https://comptox.epa.gov/dashboard/chemical-lists/CCL5PFAS> (accessed 4 April 2025); **2025**. Published online.
- Leung SCE, Wanninayake D, Chen D, Nguyen NT, Li Q. , Physicochemical properties and interactions of perfluoroalkyl substances (PFAS) - Challenges and opportunities in sensing and remediation. *Sci. Total Environ.* **2023**, *905*, 166764. doi: [10.1016/j.scitotenv.2023.166764](https://doi.org/10.1016/j.scitotenv.2023.166764)
- Salvatore D, Mok K, Garrett KK, et al. , Presumptive Contamination: A New Approach to PFAS Contamination Based on Likely Sources. *Environ. Sci. Technol. Lett.* **2022**, *9*, 983–990. doi: [10.1021/acs.estlett.2c00502](https://doi.org/10.1021/acs.estlett.2c00502)
- Mikkonen AT, Martin J, Upton RN, et al. , Spatio-temporal trends in livestock exposure to per- and polyfluoroalkyl substances (PFAS) inform risk assessment and management measures. *Environ. Res.* **2023**, *225*, 115518. doi: [10.1016/j.envres.2023.115518](https://doi.org/10.1016/j.envres.2023.115518)
- Cordner A, Brown P, Cousins IT, et al. , PFAS Contamination in Europe: Generating Knowledge and Mapping Known and Likely Contamination with “Expert-Reviewed” Journalism. *Environ. Sci. Technol.* **2024**, *58*, 6616–6627. doi: [10.1021/acs.est.3c09746](https://doi.org/10.1021/acs.est.3c09746)
- Fenton SE, Ducatman A, Boobis A, et al. , Per- and Polyfluoroalkyl Substance Toxicity and Human Health Review: Current State of Knowledge and Strategies for Informing Future

- Research. *Environmental toxicology and chemistry* **2020**, *40*, 606–630. doi: [10.1002/etc.4890](https://doi.org/10.1002/etc.4890)
29. Panieri E, Baralic K, Dukic-Cosic D, Dordevic A, Saso L., PFAS Molecules: A Major Concern for the Human Health and the Environment. *Toxics* **2022**, *10*, 44. doi: [10.3390/toxics10020044](https://doi.org/10.3390/toxics10020044)
 30. Dickman RA, Aga DS. , A review of recent studies on toxicity, sequestration, and degradation of per- and polyfluoroalkyl substances (PFAS). *J. Hazard. Mater.* **2022**, *436*, 129120. doi: [10.1016/j.jhazmat.2022.129120](https://doi.org/10.1016/j.jhazmat.2022.129120)
 31. Meegoda JN, Bezerra De Souza B, Casarini MM, Kewalramani JA. , A review of PFAS destruction technologies. *Int. J. Environ. Res. Public Health* **2022**, *19*, 16397. doi: [10.3390/ijerph192416397](https://doi.org/10.3390/ijerph192416397)
 32. Verma S, Lee T, Sahle-Demessie E, Ateia M, Nadagouda MN. , Recent advances on PFAS degradation via thermal and nonthermal methods. *Chemical Engineering Journal Advances* **2023**, *13*, 100421. doi: [10.1016/j.ceja.2022.100421](https://doi.org/10.1016/j.ceja.2022.100421)
 33. Yang L, Chen Z, Goult CA, Schlatter T, Paton RS, Gouverneur V. , Phosphate-enabled mechanochemical PFAS destruction for fluoride reuse. *Nature* **2025**, *640*, 100–106. doi: [10.1126/science.adl1557](https://doi.org/10.1126/science.adl1557)
 34. Stockholm Convention on Persistent Organic Pollutants (POPs). <https://www.pops.int/> (accessed 4 April 2025); **2025**. Published online.
 35. European Commission, Commission Regulation (EU) 2021/1297 of 4 August 2021 amending Annex XVII to Regulation (EC) No 1907/2006 of the European Parliament and of the Council as regards perfluorocarboxylic acids containing 9 to 14 carbon atoms in the chain (C9-C14 PFCA), their salts and C9-C14 PFCA-related substances. <https://eur-lex.europa.eu/eli/reg/2021/1297/oj> (accessed 4 April 2025); **2021**. Published online.
 36. United States Environmental Protection Agency, PFAS Strategic Roadmap: EPA's Commitments to Action 2021-2024. <https://www.epa.gov/pfas/pfas-strategic-roadmap-epas-commitments-action-2021-2024> (accessed 4 April 2025); **2025**. Published online.
 37. Ng C, Cousins IT, DeWitt JC, et al. , Addressing Urgent Questions for PFAS in the 21st Century. *Environ. Sci. Technol.* **2021**, *12755–12765*. doi: [10.1021/acs.est.1c03386](https://doi.org/10.1021/acs.est.1c03386)
 38. Chaudret B, Donard O, Eisenstein O. , *The French Academy of Sciences, La pollution aux PFAS : état des lieux des connaissances et enjeux de société*; Ministry of Ecological Transition & BRGM. **2025**.
 39. Cordner A, Goldenman G, Birnbaum LS, et al. , The True Cost of PFAS and the Benefits of Acting Now. *Environ. Sci. Technol.* **2021**, *55*, 9630–9633. doi: [10.1021/acs.est.1c03565](https://doi.org/10.1021/acs.est.1c03565)
 40. *OECD Series on Risk Managementch. Reconciling Terminology of the Universe of Per- and Polyfluoroalkyl Substances: Recommendations and Practical Guidance No. 61*; OECD Publishing, Paris. **2021**. doi: [10.1787/e458e796-en](https://doi.org/10.1787/e458e796-en)
 41. Miège C, Peretti A, Labadie P, et al. , Occurrence of priority and emerging organic compounds in fishes from the Rhone River (France). *Anal. Bioanal. Chem.* **2012**, *404*, 2721–2735. doi: [10.1007/s00216-012-6187-0](https://doi.org/10.1007/s00216-012-6187-0)
 42. Han J, Kiss L, Mei H, et al. , Chemical Aspects of Human and Environmental Overload with Fluorine. *Chemical reviews* **2021**, *121*, 4678–4742. doi: [10.1021/acs.chemrev.0c01263](https://doi.org/10.1021/acs.chemrev.0c01263)
 43. Kristiansson E, Coria J, Gunnarsson L, Gustavsson M. , Does the scientific knowledge reflect the chemical diversity of environmental pollution? – A twenty-year perspective. *Environ. Sci. Policy* **2021**, *126*, 90–98. doi: [10.1016/j.envsci.2021.09.007](https://doi.org/10.1016/j.envsci.2021.09.007)
 44. Trufelli H, Palma P, Famiglini G, Cappiello A. , An overview of matrix effects in liquid chromatography-mass spectrometry. *Mass Spectrom. Rev.* **2011**, *30*, 491–509. doi: [10.1002/mas.20298](https://doi.org/10.1002/mas.20298)
 45. Jia S, Marques Dos Santos M, Li C, Snyder SA. , Recent advances in mass spectrometry analytical techniques for per- and polyfluoroalkyl substances (PFAS). *Anal. Bioanal. Chem.* **2022**, *414*, 2795–2807. doi: [10.1007/s00216-022-03905-y](https://doi.org/10.1007/s00216-022-03905-y)
 46. Munoz G, Giraudel JL, Botta F, et al. , Spatial distribution and partitioning behavior of selected poly- and perfluoroalkyl substances in freshwater ecosystems: A French nationwide survey. *Sci. Total Environ.* **2015**, *517*, 48–56. doi: [10.1016/j.scitotenv.2015.02.043](https://doi.org/10.1016/j.scitotenv.2015.02.043)
 47. Munoz G, Vo Duy S, Budzinski H, Labadie P, Liu J, Sauvé S. , Quantitative analysis of poly- and perfluoroalkyl compounds in water matrices using high resolution mass spectrometry: Optimization for a laser diode thermal desorption method. *Anal. Chim. Acta* **2015**, *881*, 98–106. doi: [10.1016/j.aca.2015.04.015](https://doi.org/10.1016/j.aca.2015.04.015)
 48. Munoz G, Duy SV, Labadie P, et al. , Analysis of zwitterionic, cationic, and anionic poly- and perfluoroalkyl surfactants in sediments by liquid chromatography polarity-switching electrospray ionization coupled to high resolution mass spectrometry. *Talanta* **2016**, *152*, 447–456. doi: [10.1016/j.talanta.2016.02.021](https://doi.org/10.1016/j.talanta.2016.02.021)
 49. Teymoorian T, Munoz G, Vo Duy S, Liu J, Sauvé S. , Tracking PFAS in Drinking Water: A Review of Analytical Methods and Worldwide Occurrence Trends in Tap Water and Bottled Water. *ACS ES&T Water* **2023**, *3*, 246–261. doi: [10.1021/acsestwater.2c00387](https://doi.org/10.1021/acsestwater.2c00387)
 50. Teymoorian T, Delon L, Munoz G, Sauvé S. , Target and Suspect Screening Reveal PFAS Exceeding European Union Guideline in Various Water Sources South of Lyon, France. *Environ. Sci. Technol. Lett.* **2025**, *12*, 327–333. doi: [10.1021/acs.estlett.4c01126](https://doi.org/10.1021/acs.estlett.4c01126)
 51. Muhammad N, Hussain I, Fu XA, et al. , A Comprehensive Review of Instrumentation and Applications in Post-Column and In-Source Derivatization for LC-MS. *Mass Spectrom. Rev.*, n/a. doi: [10.1002/mas.21930](https://doi.org/10.1002/mas.21930)
 52. Teymoorian T, Munoz G, Sauvé S. , PFAS contamination in tap water: Target and suspect screening of zwitterionic, cationic, and anionic species across Canada and beyond. *Environ. Int.* **2025**, *195*, 109250. doi: [10.1016/j.envint.2025.109250](https://doi.org/10.1016/j.envint.2025.109250)
 53. Han Y, Pulikkal VF, Sun M. , Comprehensive Validation of the Adsorbable Organic Fluorine Analysis and Performance Comparison of Current Methods for Total Per- and Polyfluoroalkyl Substances in Water Samples. *ACS ES&T Water* **2021**, *1*, 1474–1482. doi: [10.1021/acsestwater.1c00047](https://doi.org/10.1021/acsestwater.1c00047)
 54. Baqar M, Chen H, Yao Y, Sun H. , Latest trends in the environmental analysis of PFAS including nontarget analysis and EOF-, AOF-, and TOP-based methodologies. *Anal. Bioanal. Chem.* **2025**, *417*, 555–571. doi: [10.1007/s00216-024-05643-9](https://doi.org/10.1007/s00216-024-05643-9)
 55. McDonough CA, Guelfo JL, Higgins CP. , Measuring total PFASs in water: The tradeoff between selectivity and inclusivity. *Curr. Opin. Environ. Sci. Health* **2019**, *7*, 13–18. doi: [10.1016/j.coesh.2018.08.005](https://doi.org/10.1016/j.coesh.2018.08.005)
 56. Togola A. , Note d'information sur les enjeux analytiques concernant le paramètre « Total PFAS » – Rapport AQUAREF 2023; Ministry of Ecological Transition & BRGM. **2023**.
 57. Abragam A. , *The Principles of Nuclear Magnetism*, 0–618; Oxford Science. **1983**.
 58. Claridge TD. , High-Resolution NMR Techniques in Organic Chemistry., Tetrahedron Organic Chemistry Series. Elsevier, **2009**
 59. Günther H. , *NMR Spectroscopy: Basic Principles, Concepts and Applications in Chemistry*; Wiley-VCH. 3rd ed. **2013**.
 60. International Organization for Standardization (ISO) *Quantitative nuclear magnetic resonance spectroscopy — Purity determination of organic compounds used for foods and food products — General requirements for 1H NMR internal standard method*. ISO 24583; **2021**.
 61. Dolbier WR. , *Guide to Fluorine NMR for Organic Chemists*, i-348; John Wiley & Sons, Ltd. **2016**. doi: [10.1002/9781118831106](https://doi.org/10.1002/9781118831106)
 62. Smeltz MG, Clifton MS, Henderson WM, McMillan L, Wetmore

- BA. , Targeted Per- and Polyfluoroalkyl substances (PFAS) assessments for high throughput screening: Analytical and testing considerations to inform a PFAS stock quality evaluation framework. *Toxicol. Appl. Pharm.* **2023**, *459*, 116355. doi: [10.1016/j.taap.2022.116355](https://doi.org/10.1016/j.taap.2022.116355)
63. Howe PW. , Recent developments in the use of fluorine NMR in synthesis and characterisation. *Prog. Nucl. Mag. Res. Sp.* **2020**, *118–119*, 1-9. doi: [10.1016/j.pnmrs.2020.02.002](https://doi.org/10.1016/j.pnmrs.2020.02.002)
64. Assemat O, Antoine M, Fourquez JM, et al. , ^{19}F nuclear magnetic resonance screening of glucokinase activators. *Anal. Biochem.* **2015**, *477*, 62–68. doi: [10.1016/j.ab.2015.02.006](https://doi.org/10.1016/j.ab.2015.02.006)
65. Ikeya T, Ban D, Lee D, Ito Y, Kato K, Griesinger C. , Solution NMR views of dynamical ordering of biomacromolecules. *Biochim. Biophys. Acta, Gen. Subj.* **2018**, *1862*, 287–306. doi: [10.1016/j.bbagen.2017.08.020](https://doi.org/10.1016/j.bbagen.2017.08.020)
66. Gronenborn AM. , Small, but powerful and attractive: ^{19}F in biomolecular NMR. *Structure* **2022**, *30*, 6–14. doi: [10.1016/j.str.2021.09.009](https://doi.org/10.1016/j.str.2021.09.009)
67. Dalvit C, Ardini E, Flocco M, Fogliatto GP, Mongelli N, Veronesi M. , A General NMR Method for Rapid, Efficient, and Reliable Biochemical Screening. *J. Am. Chem. Soc.* **2003**, *125*, 14620–14625. doi: [10.1021/ja038128e](https://doi.org/10.1021/ja038128e)
68. Dalvit C, Vulpetti A. , Ligand-Based Fluorine NMR Screening: Principles and Applications in Drug Discovery Projects. *J. Med. Chem.* **2018**, *62*, 2218–2244. doi: [10.1021/acs.jmedchem.8b01210](https://doi.org/10.1021/acs.jmedchem.8b01210)
69. Okaru AO, Brunner TS, Ackermann SM, et al. , Application of ^{19}F NMR Spectroscopy for Content Determination of Fluorinated Pharmaceuticals. *Journal of Analytical Methods in Chemistry* **2017**, *2017*, 9206297. doi: [10.1155/2017/9206297](https://doi.org/10.1155/2017/9206297)
70. Yamazaki T, Saito T, Ihara T. , A new approach for accurate quantitative determination using fluorine nuclear magnetic resonance spectroscopy. *J. Chem. Metrol.* **2017**, *11*, 16–22. doi: [10.25135/jcm.3.17.03.036](https://doi.org/10.25135/jcm.3.17.03.036)
71. Moody CA, Kwan WC, Martin JW, Muir DCG, Mabury SA. , Determination of Perfluorinated Surfactants in Surface Water Samples by Two Independent Analytical Techniques: Liquid Chromatography/Tandem Mass Spectrometry and ^{19}F NMR. *Anal. Chem.* **2001**, *73*, 2200–2206. doi: [10.1021/ac0100648](https://doi.org/10.1021/ac0100648)
72. Camdzic D, Dickman RA, Aga DS. , Total and class-specific analysis of per- and polyfluoroalkyl substances in environmental samples using nuclear magnetic resonance spectroscopy. *Journal of hazardous materials letters* **2021**, *2*, 100023. doi: [10.1016/j.hazl.2021.100023](https://doi.org/10.1016/j.hazl.2021.100023)
73. Camdzic D, Dickman RA, Joyce AS, Wallace JS, Ferguson PL, Aga DS. , Quantitation of Total PFAS Including Trifluoroacetic Acid with Fluorine Nuclear Magnetic Resonance Spectroscopy. *Analytical chemistry* **2023**, *95*, 5484–5488. doi: [10.1021/acs.analchem.2c0534](https://doi.org/10.1021/acs.analchem.2c0534)
74. Gauthier JR, Mabury SA. , Noise-Reduced Quantitative Fluorine NMR Spectroscopy Reveals the Presence of Additional Per- and Polyfluorinated Alkyl Substances in Environmental and Biological Samples When Compared with Routine Mass Spectrometry Methods. *Analytical chemistry* **2022**, *94*, 3278–3286. doi: [10.1021/acs.analchem.1c05107](https://doi.org/10.1021/acs.analchem.1c05107)
75. Gauthier JR, Mabury SA. , Identifying Unknown Fluorine-Containing Compounds in Environmental Samples Using ^{19}F NMR and Spectral Database Matching. *Environ. Sci. Technol.* **2023**, *57*, 8760–8767. doi: [10.1021/acs.est.3c01220](https://doi.org/10.1021/acs.est.3c01220)
76. Keeler J. , Understanding NMR Spectroscopy; Apollo - University of Cambridge Repository. **2002**. doi: [10.17863/CAM.968](https://doi.org/10.17863/CAM.968)
77. Malliaiv TE, Desvaux H, Delsuc MA. , Conditions for the measurement of quantitative off-resonance ROESY intensities. *Magn. Reson. Chem.* **1998**, *36*, 801–806. doi: [10.1002/\(SICI\)1097-458X\(1998110\)36:11<801::AID-OMR367>3.0.CO;2-J](https://doi.org/10.1002/(SICI)1097-458X(1998110)36:11<801::AID-OMR367>3.0.CO;2-J)
78. Kunz D. , Use of frequency-modulated radiofrequency pulses in MR imaging experiments. *Magnet. Reson. Med.* **1986**, *3*, 377–384. doi: [10.1002/mrm.1910030303](https://doi.org/10.1002/mrm.1910030303)
79. Bohlen J, Bodenhausen G. , Experimental Aspects of Chirp NMR Spectroscopy. *Journal of Magnetic Resonance, Series A* **1993**, *102*, 293–301. doi: [10.1006/jmra.1993.1107](https://doi.org/10.1006/jmra.1993.1107)
80. Cano KE, Smith MA, Shaka A. , Adjustable, Broadband, Selective Excitation with Uniform Phase. *J. Magn. Reson.* **2002**, *155*, 131–139. doi: [10.1006/jmre.2002.2506](https://doi.org/10.1006/jmre.2002.2506)
81. Power JE, Foroozandeh M, Adams RW, et al. , Increasing the quantitative bandwidth of NMR measurements. *Chem. Commun.* **2016**, *52*, 2916–2919. doi: [10.1039/c5cc10206e](https://doi.org/10.1039/c5cc10206e)
82. Khaneja N. , Chirp excitation. *J. Magn. Reson.* **2017**, *282*, 32–36. doi: [10.1016/j.jmr.2017.07.003](https://doi.org/10.1016/j.jmr.2017.07.003)
83. Coote P, Bermel W, Arthanari H. , Optimization of phase dispersion enables broadband excitation without homonuclear coupling artifacts. *Journal of magnetic resonance* **2021**, *325*, 106928. doi: [10.1016/j.jmr.2021.106928](https://doi.org/10.1016/j.jmr.2021.106928)
84. Battiste J, Newmark RA. , Applications of ^{19}F multidimensional NMR. *Prog. Nucl. Mag. Res. Sp.* **2006**, *48*, 1–23. doi: [10.1016/j.pnmrs.2005.10.002](https://doi.org/10.1016/j.pnmrs.2005.10.002)
85. Aspers RL, Ampt KA, Dvortsak P, Jaeger M, Wijmenga SS. , Fluorine detected 2D NMR experiments for the practical determination of size and sign of homonuclear F–F and heteronuclear C–F multiple bond J-coupling constants in multiple fluorinated compounds. *J. Magn. Reson.* **2013**, *231*, 79–89. doi: [10.1016/j.jmr.2013.03.008](https://doi.org/10.1016/j.jmr.2013.03.008)
86. Luy B. , Fast Pulsing 2D NMR Methods. In: *Fast 2D Solution-state NMR: Concepts and Applications*, , The Royal Society of Chemistry, **2023**
87. Claridge TD. , Chapter 5 – Correlations through the chemical bond I: Homonuclear shift correlation. In: *High-Resolution NMR Techniques in Organic Chemistry*, , Tetrahedron Organic Chemistry Series. Elsevier, **2009**, 129–188
88. Gibbs SJ, Johnson CS. , A PFG NMR experiment for accurate diffusion and flow studies in the presence of eddy currents. *Journal of Magnetic Resonance (1969)* **1991**, *93*, 395–402. doi: [10.1016/0022-2364\(91\)90014-k](https://doi.org/10.1016/0022-2364(91)90014-k)
89. Johnson C. , Diffusion ordered nuclear magnetic resonance spectroscopy: principles and applications. *Prog. Nucl. Mag. Res. Sp.* **1999**, *34*, 203–256. doi: [10.1016/S0079-6565\(99\)00003-5](https://doi.org/10.1016/S0079-6565(99)00003-5)
90. Ernst RR, Anderson WA. , Application of Fourier Transform Spectroscopy to Magnetic Resonance. *Rev. Sci. Instrum.* **1966**, *37*, 93–102. doi: [10.1063/1.1719961](https://doi.org/10.1063/1.1719961)
91. Harris RK, Becker ED, Menezes dSMC, Goodfellow R, Granger P. , NMR nomenclature. Nuclear spin properties and conventions for chemical shifts(IUPAC Recommendations 2001). *Pure Appl. Chem.* **2001**, *73*, 1795–1818. doi: [10.1351/pac200173111795](https://doi.org/10.1351/pac200173111795)
92. Cherni A, Chouzenoux E, Delsuc MA. , PALMA, an improved algorithm for DOSY signal processing. *The Analyst* **2017**, *142*, 772–779. doi: [10.1039/c6an01902a](https://doi.org/10.1039/c6an01902a)
93. Chiron L, Coutoully MA, Starck JP, Rolando C, Delsuc MA. , SPIKE a Processing Software dedicated to Fourier Spectroscopies. *arXiv (Cornell University)* **2016**. doi: [10.48550/arxiv.1608.06777](https://doi.org/10.48550/arxiv.1608.06777)
94. Margueritte L, Markov P, Chiron L, et al. , Automatic differential analysis of NMR experiments in complex samples. *Magn. Reson. Chem.* **2018**, *56*, 469–479. doi: [10.1002/mrc.4683](https://doi.org/10.1002/mrc.4683)
95. Margueritte L, Duciel L, Bourjot M, Vonthon-Sénécheau C, Delsuc MA. , Automatised pharmacophoric deconvolution of plant extracts – application to Cinchonabark crude extract. *Faraday discussions* **2019**, *218*, 441–458. doi: [10.1039/c8fd00242h](https://doi.org/10.1039/c8fd00242h)
96. U.S. Food and Drug Administration, Per and Polyfluoroalkyl Substances (PFAS) in Cosmetics. <https://www.fda.gov/cosmetics/cosmetic-ingredients-and-polyfluoroalkyl-substances-pfas-cosmetics> (accessed 17 June 2024); **2024**. Published online.
97. Bingol K. , Recent advances in targeted and untargeted

- metabolomics by NMR and MS/NMR methods. *High Throughput* **2018**, *7*, 9. doi: [10.3390/ht7020009](https://doi.org/10.3390/ht7020009)
98. Cajka T, Fiehn O., Toward Merging Untargeted and Targeted Methods in Mass Spectrometry-Based Metabolomics and Lipidomics. *Anal. Chem.* **2016**, *88*, 524-545. PMID: 26637011 doi: [10.1021/acs.analchem.5b04491](https://doi.org/10.1021/acs.analchem.5b04491)

Supporting information

Additional supporting information may be found in the online version of the article at the publisher's website.